POLITECNICO
MILANO 1863

SPACE ENGINEERING

Space System Engineering and Operations

MARS EXPRESS MISSION:
reverse engineering analysis

Team 32

11/09/2022

Space Engineering
Space System Engineering and Operations

Title:
MARS EXPRESS MISSION:
reverse engineering analysis

Abstract:

The aim of this work is to analyse the Mars Express (MEX) mission focusing on the mission analysis and on the main subsystem of the spacecraft to understand and motivate the choice and the design adopted in the mission. A reverse engineering process it is performed: the mission budgets and the design at subsystem level are compared, discussed and verified through quantitative sizing. Finally the high level mission and technical requirements are extracted.

Project group:

Team 32

Students:

Bruno Falò	100861
Francesca Tozzini	996623
Gloria Castronovo	992130
Federico Infantino	996989
Mads L. U. Larsen	984967
Francesco Salvaterra	988375

Professor:

Prof. Michèle Roberta Lavagna

Academic year:

2021-2022

Preface

This work focuses on the ESA Mars Express mission, launched in 2003, to study the planet Mars.

First a brief overview of what the mission is, as well as its objectives, the correlate functional analysis and the scientific payload carried on, are proposed. In addition, a brief discussion about the environment encountered by the probe and a mission analysis are presented. In more detail, an analysis is carried out from the engineering point of view of the phases into which the mission is divided, the trajectory adopted and the choice of the actual orbit.

After that, the main subsystems that make up the spacecraft are presented: propulsion subsystem, attitude and orbital control subsystem, TMT&TC subsystem, electric power subsystem, thermal control subsystem and structure and configuration. After a brief discussion about the real solutions adopted, an inverse engineering method is implemented: the mission budgets and the design at subsystem level are compared, discussed and verified through quantitative sizing. Finally, for each subsystem, the high-level mission and technical requirements are obtained.

Nomenclature

Abbreviations

ADCS Attitude Determination and Control Subsystem

AGS Air Gassing System

COM Centre Of Mass

DOD Depth Of Discharge

EDLS Entry Descent Landing System

GAP Gas Analysis Package

IMU Inertia Measurement Unit

LVA Launch Vehicle Adapter Ring

MELACOM Mars Express Lander Communication

MLI Multi-layer insulation

NCPV Normally Closed Pyrotechnic Valve

PAW Position Adjustable Workbench

UHF Ultra High Frequency

BCR Battery Charge Regulator

BER Bit Error Rate

BOL Beginning Of Life

C&DH Command & Data Handling

CDMU Control & Data Management Unit

DSN Deep Space Network

EIRP Equivalent Isotropic Radiated Power

EOL End Of Life

EPS Electric Power Subsystem

FCL Foldback Current Limiter

HGA High Gain Antenna

IMU Inertial Measurement Unit

LCL Latch Current Limiter

LGA Low Gain Antenna

MEX Mars Express

PDU Power Distribution Unit

PPT Peak-Power Tracker

RW Reaction Wheel

s/c Spacecraft

SADM Solar Array Drive Mechanism

SNR Signal to Noise Ratio

SSPA Solid State Power Amplifer

STR Star Tracker

TCM Trajectory Correction Manoeuvre

TMT&TC Telemetry, Tracking, and Telecommunications

TWTA Traveling wave tube amplifier

Symbols

α Solar aspect angle

ΔV Cost of a manoeuvre

$\Delta V_{3stages}$ Increment of velocity - launcher

ΔV_{Fregat} Increment of velocity - Fregat

ΔV_{TOT} Cost of a sequence of manoeuvre

η Cell efficiency

λ Wavelength

μ Planetary constant

μ_{amp} Amplifier efficiency

ν_{pl}	Inclination angle between planet and s/c
ν_{sun}	Inclination angle between sun and s/c
σ	Boltzmann Constant
Θ_{rx}	Half-power beam width
A_{ill}	Spacecraft area subjected to solar radiation
A_{sa}	Solar arrays area
B	Mars magnetic field at spacecraft altitude
B_0	Mars magnetic field
B_{dB}	Signal Bandwidth
C_{cap}	Channel Capacity
C_g	Centre of mass
C_{ps}	Centre of solar radiation pressure
C_{real}	Actual capacity of the battery
C_r	Capacity of the battery
C_{string}	Capacity of one string of cells
D	Residual dipole of the spacecraft
d	Degradation factor
D_{rx}	Diameter of receiver
D_{tx}	Diameter of transceiver
E_d	Battery density per unit mass
E_v	Battery density per unit volume
f	Frequency
g_0	earth gravitational acceleration at surface
G_{rx}	Gain receiver
G_{tx}	Gain transceiver
H	Vehicle angular momentum
h	Orbital semi-major axis
I_s	Specific impulse
I_x, I_y, I_z	Inertia axis
I_d	Inherent losses
k	Boltzmann constant
L	Distance between thrusters
$L_{c,a,p,s}$	Signal loss - Cable, Atmospheric, Pointing, Space
N_0	System noise density
$N_{cell_{TOT}}$	Total number of solar cells
N_{ser}	Number of cells in series
N_{string}	Number of strings
P_c	Power Carrier
P_0	Solar cell specific power
P_{BOL}	solar arrays power at BOL
P_d	Maximum daylight power demand
P_{EOL}	Solar array power at EOL
P_e	Maximum eclipse power demand
P_{rx}	Power receiver
P_{sa}	Solar array power required
P_{tx}	Power transceiver
q	Reflectivity coefficient
Q_{albedo}	Heat from planet albedo
q_{albedo}	Heat flux from planet albedo
Q_{emi}	Heat emitted from S/c
Q_{int}	Internal S/c Heat
Q_{IR}	Infrared Heat from planet
q_{IR}	Infrared Heat flux from planet
q_o	Heat flux from sun
Q_{Sun-sc}	Heat from sun onto spacecraft
q_{Sun-sc}	Heat flux from sun onto spacecraft

R	Rate of Charge
R_0	Mars radius
R_d	Date Rate
R_M	Mars radius
R_{orbit}	Orbit radius
R_{orbit}	S/c orbital radius
R_{pl}	Planet radius
T	Orbital period
T_m	Magnetic torque
T_s	Sensor temperature
T_s	Solar radiation Torque
T_d	Sunlight duration
T_e	Eclipse duration
T_{gx}	Gravitational torque around the x axis
T_{sc}	Temperature of S/c
V_{real}	Real output voltage from solar arrays
X_d	Daylight efficiency factor
X_e	Eclipse efficiency factor

Contents

Introduction 1

This chapter will present a brief explanation of the Mars Express (MEX) mission, this will include a short mission overview, a presentation of the scientific- and mission objectives, and a brief scientific payload description. This chapter is based on the information given in Wilson (2004)
MEX was the first ESA mission to Mars, it included both an orbiter and a small lander named Beagle 2 (Appendix A). The main objectives was the global study of the planet using science instruments onboard.

1.1 Mission Overview

The following section is based on information given in Chicarro, Martin, and Trautner (2004). On the 2nd of June 2003 the 1223 kg Mars Express was launched and injected into a Mars transfer orbit, using a Soyuz rocket with a Fregat upper stage. MEX is dedicated to the orbital and in-situ study of the planet's interior, subsurface, surface, and atmosphere. It was placed in an elliptical orbit, which was optimized for the scientific objective and to communicate with Beagle 2. The orbit details are presented in Table 1.1.

Apoapsis	Periapsis	inclination (i)	Period T
10 142 km	250 km	86.35°	6.75 h

Table 1.1: MEX orbit insertion parameters

The spacecraft was captured into Mars orbit in the 25th of December 2003, the spacecraft finished its own commissioning in mid-January 2004, hereafter the experiments started their own commissioning and started gathering data from Mars and its environment. The optical instruments started their routine operations in June 2004. The nominal orbiter lifetime is a martian year (687 days), following Mars orbit insertion and about 7 months' cruise.

The Beagle 2 descent capsule was ejected 5 days before arrival at Mars, it entered and descended through the atmosphere in about 5 min., intended to land at $< 40\,\mathrm{m\,s^{-1}}$ within an error ellipse of 20×100 km. The Beagle 2 operational lifetime was about 6 months, but no signal was ever received from the lander.

1.2 Mission understanding, objectives identification and analysis

The **Mars Express** mission is dedicated to the orbital (and originally in-situ) study of the interior, subsurface, surface and atmosphere, and environment of the planet Mars. The scientific objectives of the Mars Express mission represent an attempt to fulfill in part the lost scientific goals of the Russian Mars 96 mission, complemented by exobiology research with the lander **Beagle-2**. Mars exploration is crucial for a better understanding of the Earth from the perspective of comparative planetology. The spacecraft originally carried seven scientific instruments, a small lander, a lander relay and a Visual Monitoring Camera, all designed to contribute to solving the mystery of Mars' missing water. All of the instruments take measurements of the surface, atmosphere and interplanetary media, from the main spacecraft in polar orbit, which will allow it to gradually cover the whole planet. Mars Express consists of two parts, the Mars Express Orbiter and Beagle 2, a lander designed to perform exobiology and geochemistry research, investigating the current presence of ice or liquid water in the martian crust, and possible traces of past or present biological activity on the planet. Although the lander failed to fully deploy after it landed on the Martian surface, the orbiter has been successfully performing scientific measurements since early 2004, namely, high-resolution imaging and mineralogical mapping of the surface, radar sounding of the subsurface structure down to the permafrost, precise determination of the atmospheric circulation and composition, and study of the interaction of the atmosphere with the interplanetary medium.

The primary scientific objectives of the orbiter are:

- global color and stereo high-resolution imaging with about 10 m resolution and imaging of selected areas at $2\,\mathrm{m\,px^{-1}}$.
- Global IR mineralogical mapping of the surface.
- Radar sounding of the subsurface structure down to the permafrost.
- Global atmospheric circulation and mapping of the atmospheric composition.
- Interaction of the atmosphere with the surface and the interplanetary medium.
- Radio science to infer critical information on the atmosphere, ionosphere, surface and interior.

The scientific objective of Beagle 2 was the detection of extinct and/or extant life on Mars, as well as establish if the landing site conditions were suitable for life.

1.2.1 Mission objectives design implications

The need of a Mars study from a 360-degrees perspective, requires a huge set of various and complex instruments. Mars Express is a 3-axis stabilised orbiter with a fixed high-gain antenna and body-mounted instruments, and is dedicated to the orbital and in-situ study of the planet's interior, subsurface, surface and atmosphere. It was placed in an elliptical orbit (250 x 10 142 km) around Mars of 86.35° quasi-polar inclination and 6.75 h period, which was optimised for the scientific objectives and to communicate with Beagle 2 and the NASA landers or rovers being launched in 2003-2005. One of the main primary objectives is the deep analysis of the entire environment of Mars: from a chemical point of view of the molecular composition of the atmosphere, to local geo-morphological analysis

of the landing site by Beagle-2 also using high resolutions camera. The need of complete analysis of the martian environment through the instruments of the spacecraft, requires also an highly elliptical orbit with a perigee of 270 km above the surface this allows to have a wide coverage of the surface, good communication with Beagle 2 and to obtain high resolution images. On 2 June 2003 Mars Express was launched from Baikonur and injected into a Mars transfer orbit.

Launch windows to Mars occur every 26 months but 2003 was particularly favourable because it offered a short interplanetary voyage.

The Beagle 2 descent capsule, as mentioned before, was ejected 5 days before arrival at Mars, while the orbiter was on a Mars collision course; Mars Express was then retargeted for orbit insertion.

The spacecraft was captured into Mars orbit in late December 2003 and it started the operations in January 2004.

The radar antenna was planned to be deployed last in order to maximise early daylight operations of the other instruments, . The deployment of the radar antennas was delayed for safety modelling checks. Other instruments were used in June 2004. The nominal orbiter mission lifetime was planned to be a martian year (687 days); the mission is currently active.

1.2.2 Instruments

The MEX orbiter science payload totals 116 kg and consists of six instruments and a radio-science experiment. They are divided into two categories, those dealing with surface and subsurface observation, and those studying the atmosphere and environment of Mars.

1.2.2.1 HRSC - The High Resolution Stereo Camera

The major goal of this instrument is global coverage of Mars in high resolution, with the science data focusing on the role of water and climate throughout martian history, the timing and evolution of volcanism and tectonics, the surface/atmosphere interactions, the establishment of an accurate chronology, and the observation of Phobos and Deimos. In order to meet these objectives the the HRSC allows for the characterisation of surface features and morphology at high spacial resolution($10\,\mathrm{m\,px^{-1}}$ in stereo), surface topography at high spatial and vertical resolution, surface features and morphology using super resolution ($2\,\mathrm{m\,px^{-1}}$). The high- and super-resolution are obtained around pericenter, at and above 250 km.

1.2.2.2 OMEGA - Observatoire pour la Minéralogie, l'Eau, les Glaces et l'Activité

This is a visible and near-IR mapping spectrometer operating in the wavelengths range 0.38 µm - 5.1 µm. It will provide global coverage of Mars with a resolution of 1 km - 5 km by the end of the nominal mission from altitudes between 1000 km and 4000 km, and selected areas will have high-resolution (a few hundred meters) snapshot amounting to a few percent of the surface. OMEGA will characterise the composition of surface materials,

studying the time and space distribution of atmospheric CO_2, CO and H_2O, and analysing dust particles on the surface and atmosphere.

1.2.2.3 MARSIS - Mars Advanced Radar for Subsurface and Ionosphere Sounding

MARSIS is a low-frequency nadir looking pulse-limited radar sounder and altimeter with ground-penetrating capabilities. It uses two 20 m booms and a secondary receiving monopole antenna to isolate the subsurface reflections. The primary objective is to map the distribution of water in the upper portions of the crust, down to 3 km - 5 km. The detection of such water reservoirs will help to investigate the evolution of Mars. Secondary objectives include subsurface geologic probing, surface roughness and topography characterisation, and ionosphere sounding to characterise the interactions of the solar wind with the ionosphere and the upper atmosphere.

1.2.2.4 PFS - The Planetary Fourier Spectrometer for Mars Express

The PFS is an IR spectrometer optimized for atmospheric studies, it covers the wavelength ranges 1.2 µm - 45 µm with a spectral resolution of $2\,cm^{-1}$ and a spacial resolution of 10 km - 20 km. The primary scientific objective is the global long-term monitoring of 3-D temperature field in the lower atmosphere, the measurement of the minor constituent variations (water vapour and carbon monoxide) and D/H ratio, the determination of the size distribution, chemical composition and optical properties of the atmospheric aerosols, dust clouds, ice clouds and hazes, and the study of global circulation and dynamics.

1.2.2.5 SPICAM - Studying the Global Structure and Composition of the Martian Atmosphere

SPICAM is a UV and IR spectrometer which main objective is studying atmospheric photo-chemistry, the density-temperature structure of the atmosphere (0-150 km), the upper atmosphere-ionosphere escape processes, and the interaction with the solar wind. The UV sensor is looking through the atmosphere either at the Sun or stars to obtain vertical profiles by occultation, or to the nadir to obtain integrated profiles, or at the limb to obtain vertical profiles of high-atmosphere emissions. The IR sensor is used only in the nadir-looking mode.

1.2.2.6 ASPERA-3 - Analyser of Space Plasma and Energetic Ions for Mars Express

ASPERA is a energetic neutral atom analyser which primary objective is studying plasma domains at different locations along the spacecraft's orbit, focusing on the interaction of the upper atmosphere with the interplanetary medium and the solar wind, and characterising the near-Mars plasma and neutral gas environment. In-situ measurements of ions and electrons complement the energetic neutral atom images, they provide undisturbed solar wind parameters.

1.2.2.7 MaRS - Mars Express Orbiter Radio Science

MaRS is performing radio sounding experiments of the neutral martian atmosphere and ionosphere to derive vertical density, pressure, and temperature profiles as a function of height, and the diurnal and seasonal variations in the ionosphere. It is also determining the dielectric and scattering properties of the martian surface in specific target areas with a bistatic radar experiment, and is determining gravity anomalies in the crust in order to investigate the structure and evolution of the interior. Precise determination of the mass of Phobos and radio sounding of the solar corona during superior conjunction with the Sun are also among the objectives. The experiment relies on the observation of the phase, amplitude, polarisation and propagation times of radio signals transmitted by the spacecraft and received at ground stations on Earth.

1.3 Payload design effects

The scientific instruments carried on the Orbiter impose some constrain in order to carry out their task, such as:

- HRSC, SPICAM, OMEGA, PFS should be nadir-pointing instruments and attached to the same panel for coalignment purpose. This also cope with thermal constraints related to the orientation of their heat pipes and with the proximity of the s/c thermal radiators
- Instruments sensible to Sun radiation should be mounted such a way that in nominal condition they never seen the sun, so perpendicular with respect to the solar panels
- Instruments should be aligned with the launch direction to ensure compatibility with thruster plume impingement (and any eventual aerobraking)
- Instrument view should be in the anti-ram direction during low-altitude passes through the Martian atmosphere in order to avoid the direct impact with the particles that can affect the proprieties of the instruments .
- The choice of the shape of the orbit should be compatible with the operating condition of the instruments
- The memory and the OBDH subsystem shall be sized properly to be able to manage the huge quantity of scientific data coming from the instruments (also telemetry data to consider). This may lead to an increment of the system mass meaning more propellant and higher costs.
- The huge amount of data to transmit also affect the duration of each time window, the transmission, and in particular the short operational windows

1.4 Spacecraft and Instrument data

The following section will present the relevant data used to perform subsystem preliminary sizing and estimation. All data are from ESA (2022b) and Wilson (2004).

Mass Budget	
	Mass at launch [kg]
Spacecraft Bus	439
Lander	71
Payload	116
Propellant	427
Launch mass	1223

Table 1.2: Mass budget from ESA (2022b).

Power Budget			
	Typical mean power demand		
	Observation [W]	Manoeuvre [W]	Communication [W]
Spacecraft	270	310	445
Payload	140	50	55
Total	410	360	500

Table 1.3: Mean power budget from ESA (2022b).

Dimensions	
Spacecraft Bus	$1.5\,\mathrm{m} \times 1.8\,\mathrm{m} \times 1.4\,\mathrm{m}$
Main engine thrust	$400\,\mathrm{N}$
Attitude thrusters	8 at $10\,\mathrm{N}$ each
Propellant tanks volume	$2 \times 270\,\mathrm{L} = 540\,\mathrm{L}$
Pointing accuracy	$< 0.05°$

Table 1.4: Dimensions from ESA (2022b).

Power Source	
Solar array area	$11.42\,\mathrm{m}^2$
Lithium batteries	3 at $22.5\,\mathrm{A}$

Table 1.5: Power sources from ESA (2022b)

Thermal Specification	
Spacecraft	$10\,°\mathrm{C}$ - $20\,°\mathrm{C} \pm 15\,°\mathrm{C}$
PFS and OMEGA	$-180\,°\mathrm{C}$
Thermal Blanket	Glod-plated AISn alloy

Table 1.6: Thermal specifications from ESA (2022b)

	Mass [kg]	Power consumption	Data output	Operational lifetime
HRSC (SRC)	19.6	45.7 W (3 W)	peak 25 Mbit s^{-1} $\approx$ 1 Gbit day^{-1}	> 4 years
OMEGA	28.8	47.6 W peak (27.4 W cooling)	200 Mbit $session^{-1}$	>2500 h
MARSIS	17	max 64.5 W	285 Mbit day^{-1}	-
PFS	31.2	35 W nominal (44 W peak)	250 Mbit day^{-1}	-
SPICAM	4.7	18 W	10 MB day^{-1}	-
ASPERA-3	8.2	13.5 W	-	-
MaRS	-	65 W	-	-

Table 1.7: Relevant data for different instruments. (Wilson, 2004)
OMEGA has 3 different kinds of observing sessions dependant on altitude.

1.5 Functional analysis

The scientific objectives of the mission, as stated in "ESA's Mars Express Mission– Europe on Its Way to Mars" n.d., are: "The remote and in-situ study of the surface, subsurface atmosphere and environment of the planet Mars", while maintaining overall mission cost below a very stringent cost cap. We can thus obtain the driver of the mission: perform scientific observations while maintaining the costs low during development. From these general objectives, performing a first step of functional analysis, we can derive the main functionalities of the mission:

- Launch from the Earth's surface and inject into an interplanetary trajectory.
- Perform the interplanetary trajectory and reach Mars' orbit.
- Inject into a correct orbit to perform science.
- Correctly maintain the orbit and attitude for the duration of the whole mission.
- Manage a correct separation and landing of the Lander/Landers.
- Perform remote sensing from orbit.
- Perform in-situ sensing from ground.

All these aspects are needed and derived from the given scientific objectives. The first five aspects refer to all the necessary phases and modes the mission must accomplish to reach the planet Mars and maintain the orbit required by the payload, while the last two aspects derive directly from the requisites of the mission. As the objectives require in-situ scientific operations, one or multiple landers are needed and thus all phases that enable their correct deployment and communication with it/them. This aspect profoundly influences other mission aspects such as the orbital parameters of the spacecraft and its structure.

Important requirements that influence all the development of the mission are the low-cost cap and the necessity to accelerate the development to accommodate the 2003 launch window, these requirements impose the reuse of existing items, operational systems and exploiting all similarities with the Rosetta mission.

To perform these functions, the spacecraft needs to have the relevant functionalities assigned to the relative subsystems. Performing an additional iteration of the functional analysis, we obtain a system-level analysis.

Functionalities of the ground segment:

- Support the downlink and uplink of the data from the spacecraft.
- Manage the spacecraft and mission.

Role of the service module:

- Resist the structural loads and vibrations at the takeoff and during the whole mission.
- Perform the requested orbital transfer and orbital injections burns.
- Provide orbital maintenance.
- Provide attitude stabilization and correct pointing for the instruments.
- Provide thermal control.
- Supply the spacecraft with enough electrical power.
- Maintain communication with the ground segment.
- Maintain communication with the Lander.
- Acquire data about the correct behavior of the system.
- Perform computation for the system and payload data.
- Store commands and data.
- Automatically put itself in safe mode in case it detects an anomaly.
- Correctly separate from the lander.

Role of the payload:

- Acquire scientific data from remote sensing.
- Acquire scientific data from in-situ analysis.

Environmental analysis 2

It is important to make an environmental analysis to understand which environmental conditions the spacecraft has to face in each phase of the mission:

- LAUNCH: In this phase the spacecraft has to cope with the highest loads which can not be controlled in general, so the spacecraft has to be designed to withstand them. The launch vehicle generates random and acoustic vibrations as well as shocks, so the structure vibrates randomly because the mechanical parts are moving
- INTERPLANETARY TRAJECTORY: The spacecraft is then subjected to solar flares, due to the deformation of the magnetic field of the sun, and radiation but also further loads during course correction burns or aerobreaking procedures.
- MARS SPHERE OF INFLUENCE: The sphere of influence of this planet is important to be considered because its environment is quite harsh for many reasons: 1) The temperatures can reach dozens of degrees below zero, so a thermal control subsystem should be installed to maintain all the equipment within the allowed temperatures ranges. For more demanding units such as payload sensors, special precautions must be taken by individually insulating such components. 2) Solar radiation is very strong so the components are radiation hardened and some specific observations are performed only under specific conditions. 3) Pressure, density and temperature change with height. It is better to compare different atmospheric models to prevent from uncertainties about orbit reconstruction. 4) There are frequencies at which the sounder can not collect data properly, so it's important to choose it properly, by considering that electromagnetic radiation can not propagate through a ionized gas at frequencies below the electron plasma frequency. 5) Airdrag and torques increment the stress on the internal structure, so it's necessary to verify it to survive to such high level of stress but also that the aerodynamic configuration is stable.

Mission Analysis 3

This chapter will present an analysis of the main phases of the MEX mission and the trajectory performed with its manoeuvring budget breakdown. Than it will be presented the preliminary sizing of the subsystem with a brief discussion about design choices, trade-offs, and the necessary requirements.

3.1 Mission phases and trajectory analysis

The main phases in which it is possible to divide the MEX mission are (M. Hechler, 2005) (*Planetary Orbit Insertion – A First Success for Europe with ESA's Mars Express* 2006) (ESA, 2022b):

3.1.1 Launch and early operation phase (2 -7 June 2003)

The minimum-energy launch windows for a Martian expedition occur at intervals of approximately two years and two months (780 days is the planet's synodic period with respect to Earth) and the lowest available transfer energy varies on a roughly 16-year cycle (when the planets are aligned). Originally a one month launch window from 23 May 2003 to 21 June 2003 was envisaged. It was favourable because it offered the maximum launch mass, and moreover the Beagle 2 could not have been carried in the less favourable 2005 window. Finally the launch date was selected as 2 June 2003 and the launch took place on that date at 17:45 UTC in Baikonur cosmodrome 45.6°N 63.4°E (Kazakistan). Cost was the main driver in the selection process of the launcher. The choice of a Soyuz Launcher ($\Delta V_{3stages} \simeq 8.3$ km/s) was also linked to the flexible approach adopted by ESA. As a relatively low cost, but extremely reliable launcher it helped keeping the overall cost of the mission within the total budget. Using a more powerful ($\Delta V_{Fregat} \simeq 4.6$ km/s) and re-startable upper stage called Fregat, it increased the payload volume and mass capability that was necessary for the mission.

After launch and separation of the various stages, the spacecraft was placed into a circular parking orbit at 200 km altitude to perform a checkout of the spacecraft before the interplanetary trajectory. One hour and thirty-two minutes after launch (19:14 UTC) the Fregat stage was reignited putting the spacecraft into interplanetary space.

3.1.2 Cruise phase (7 June - 15 December 2003)

This phase mainly represents the interplanetary transfer from the Earth to Mars. The plan foresaw a period of about six weeks after launch for testing the spacecraft in flight and commissioning of the instruments. Then it was followed by a quiet flight phase during

six months, which would allow time to prepare for the Mars Orbit Insertion. During this phase several TCM should be completed to correct the spacecraft path and minimize the ΔV. This trajectory leg covered 440 million km.

3.1.3 Mars arrival and Orbit insertion phase (15 December 2003 - 28 January 2004)

The Mars approach started with a fine targeting manoeuvre at arrival day -9 days and then two days after there was the preparation for the Beagle-2 release. The lander ejection occurs at arrival-6 days on 19 December at 8:31 UTC (Beagle 2 will be separated from the spacecraft with 0.3 m/s relative velocity at 90 km altitude). The orbit before the spacecraft re-targeting manoeuvre was fixed by the lander entry conditions. On 20 December, Mars Express fired a short thruster burst (ΔV = 14 m/s) to put it into position to orbit the planet. The Orbiter was captured into a long looping orbit on 25 December at 2:47 UTC. The actual orbit injection ΔV = 800 m/s was performed at the pericentre of the incoming hyperbola to Mars. The Orbiter was captured into an highly elliptic orbit, which parameters are summarized in Table 3.1:

Apoapsis altitude	Periapsis altitude	inclination (i)
15 000 km	250 km	25°

Table 3.1: Capture orbit parameters

Then a plane change manoeuvre at the apocentre (ΔV = 125 m/s) on the 30$^{\text{th}}$ December 2003 and a sequence of manoeuvres (ΔV_{TOT} = 364 m/s) at the pericentre on 3-6-11 January 2004 injected the spacecraft into a nearly polar eccentric orbit, which parameters are collected in Table 3.2:

Apoapsis altitude	Periapsis altitude	inclination (i)	Period T
11 560 km	285 km	86.35°	7.5 h

Table 3.2: Orbit parameters after change plane manoeuvre
(R. Pischel, 2009)

The nominal orbit was reached at 28 January 2004. (M. Hechler, 2005) (*Planetary Orbit Insertion – A First Success for Europe with ESA's Mars Express* 2006)

3.1.4 Operational phase (28 January 2004 - December 2005)

The science operations phase for the Orbiter is the period of time when the spacecraft use its scientific instruments to study the Martian environment. During this phase, in August 2004 the apoapsis was lowered to 10107 km and periapsis raised to 298 km to give an orbital period of 6.7 hours in order to reach a better seasonal coverage in the polar region. The manoeuvres occurred at the periapsis passages. The new nominal orbit parameters are collected in the Table 1.1.

The choice of both the nominal orbit was dictated by the optimal observing conditions for scientific experiments, in particular:

- Coverage whole Martian surface from low altitude

- Different ground track spacing
- Different illumination conditions: about 30% night side viewing
- A relay service to the Beagle 2

These orbits have been selected such that the pericentre regression due to the J2 effect leads to optimum coverage for the combination of instruments on board, from low altitudes near pericentre, but also from high altitudes. The first operational orbit (G3-u) completes 13 revolutions each four Martian sidereal days, while the second orbit (G3-b) after the apocentre reduction, completes 11 revolutions in 3 Martian days. In absence of perturbations, after one cycle, the spacecraft ground-track would repeat. More in detail, the second apocentre reduction was performed to improve the seasonal coverage of the polar regions. In general, near periapsis, the top deck will be pointed down towards the Martian surface and near apoapsis the high gain antenna will be pointed towards Earth for uplink and downlink. The design of a Mars mission, as well as a generic planet mission, includes the **eclipse** and **occultations** (Mars is between s/c and Earth). These critical phases influence two main aspects:

- Energy consumption
- Signals transmission

During **occultations**, communications with Earth is not possible. This imposes constraints for the selection of the downlink windows withing an orbit. A significant segment of each orbit is used to turn the fixed-mounted spacecraft antenna to Earth for data downlink and command uplink. These windows cannot be used for pointed science observations. The location and duration of the downlink windows depend on the availability of ground stations. The average downlink duration per day is 8–10 hours, spread over several sessions of about three hours each.

3.1.5 Disposal

Mars Express orbiter will simply keep orbiting the planet for at least 50 years. Then it will probably burn up in Mars's atmosphere. This will also ensure that debris will not pollute the planet's surface.

3.2 Trajectory reverse engineering

3.2.1 Trajectory simulation

Reverse engineering was applied on the mission design. The launch from Baikonur to a 200km parking orbit was estimated to cost about 9.5km/s of ΔV. The parking orbit provides a safe and simple orbit to perform a satellite checkout and to match post lift off and insertion conditions. A simple interplanetary transfer to Earth parking orbit to Mars, with the same departure date and same tof was estimated to cost 5.69 km/s (calculated using a single Lambert arc approach). A better launch date was found before the actual date of departure, but the reduction of the cost found was considered negligible and probably affected by small errors, such as the absence of deep space manoeuvres in the solution. To reduce the number of flight programs implemented for the upper stage, in the real mission only 10 escape trajectories were defined and 10 days after launch the trajectory was corrected (M. Hechler, 2005). The lander was released directly by the spacecraft and

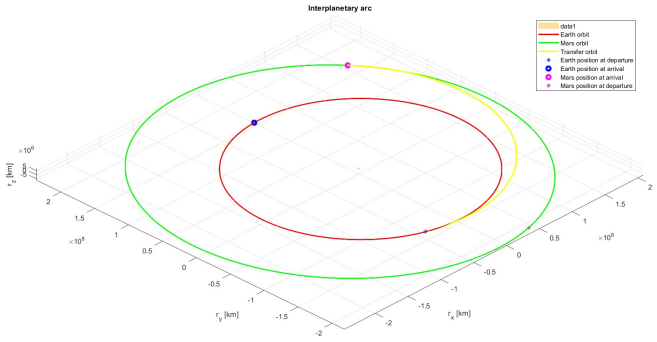

Figure 3.1: calculated interplanetary arc

then the orbit was adjusted for the incoming insertion, this was done probably to reduce the cost of the mission and improve reliability, as the lander was passive, and actuators and sensors were not implemented for the landing. The estimation of the orbit insertion was found to be 0.7627 km/s, close to the actual value of 0.8km/s (M. Hechler, 2005) and the change of plane was estimated to be 118 m/s (close to the 125m/s of the actual cost) (M. Hechler, 2005). The first change of apocentre, from 150000 km to 11560 km was estimated to cost 443 m/s, the second apocentre reduction was estimated to amount to 45 m/s. All calculations are made assuming simple maneuvers.

The ground track of the final orbit was plotted, including the J2 disturb. The vertical red line shows the spacecraft passing by its closest point to Mars, at around 250 km over the surface. This is where the observation phase takes place. Conversely, where the line is curved, the spacecraft is near the farthest point out on its elliptical orbit. This is where it performs its communication with Earth, the orbital data was obtained from M. Carranza, n.d.

The orbit selected is a frozen orbit, its peculiarity is the stability with respect to perturbations and so it requires low maintenance.

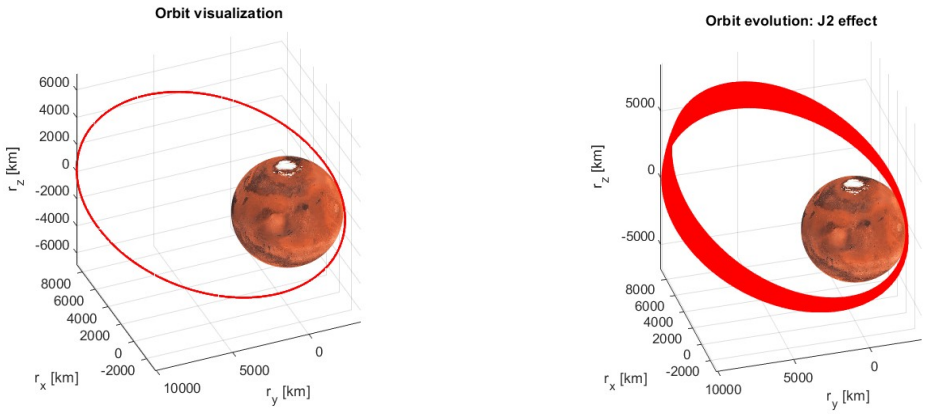

(a) Simulated orbit **(b)** Simulated orbit evolution over 1 year

Figure 3.2: orbit representations

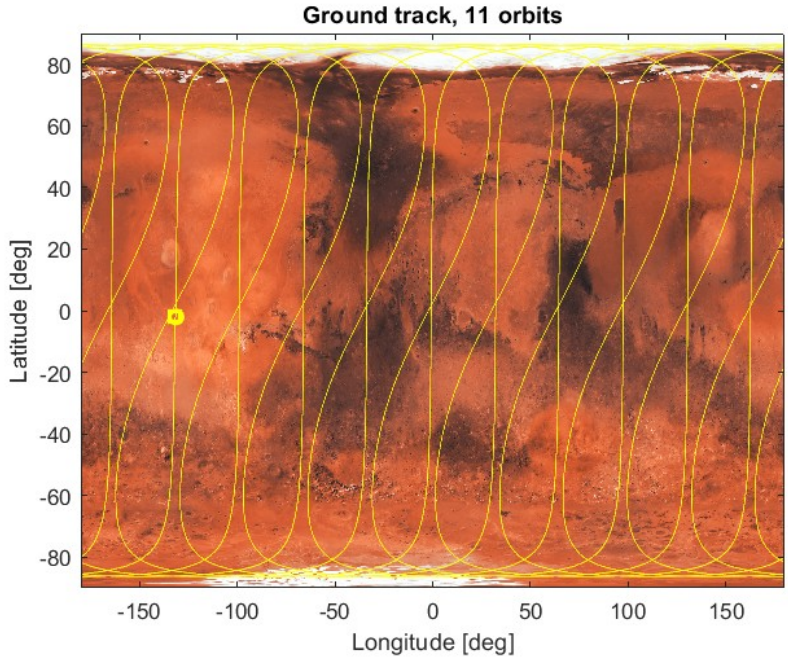

Figure 3.3: Simulated ground track

3.2.2 Trade-off analysis

Different approaches to the mission design were considered. Using the successive launch window, with departure on 2005/8/19 and arrival on 2006/3/22 with a cost of 6.79 km/s, a more traditional approach could have been used to design the mission, and more advanced technologies could have been implemented in the payload. This resulted in a greater ΔV cost of the interplanetary transfer, and increased development costs, going against the budget constraint and the objective to develop a "fast and cheap" mission.

A gravity assist with the moon was qualitatively considered (as it needs a 3-body-problem implementation since the patched conics method can not be applied). Because of the very short orbital period of the moon (27d), of which very few of them in the possible optimal position, the launch window would have been small. A delay in the launch date (for example due to weather conditions) could have been problematic.

One possible solution to the scientific objectives was a constellation of small satellites, the hypothesis was discarded as a continuous coverage of the surface is not required and the launch and maintenance of multiple satellites was deemed to be too expensive and out of the scope of the mission.

Propulsion subsystem 4

This chapter is focused on the description of the the propulsion units and architectures adopted in Mars Express mission, including the principal design aspects and the analysis of the requirements and a preliminary sizing of the propulsion unit, comparing the results with the real data get from *Chicarro, A., et al., The Mars Express Mission: An Overview, in Mars Express: The Scientific Payload, A. Wilson Ed., ESA SP-1240, European Space Agency Publications Division, Noordwijk, Netherlands, ISBN 92-9092-556-6, pp. 3-16, 2004.*.

4.1 Mars Express Propulsion subsystem overview

Most of the energy needed to propel Mars Express from Earth to Mars was provided by the three-stage Soyuz/Fregat launcher. The Fregat upper stage separated from the spacecraft after placing it on a Mars-bound trajectory. The spacecraft used its on-board means of propulsion solely for orbit corrections and to slow the spacecraft down for Mars orbit insertion. The first three stages of Soyuz + Fregat were used to to put the spacecraft in the circular orbit and then from the circular to the interplanetary transfer.

4.1.1 Propulsion units and architecture

The spacecraft propulsion configuration included a Main Engine (414 N) which was used to perform all the major trajectory changes, and 10 N thrusters used for the attitude control and also to produce the thrust during the small trajectory corrections. The 10 N thrusters configuration was optimised to perform all the attitude control functions with only 4 redunded thrusters, each of them being implemented near a corner of the -Z face of the spacecraft.

Propulsion units

Unit	Thrust[N]
Main Engine	400
8 AOCS thrusters	10 each

Table 4.1: Propulsion units from esa.int ESA (2022b).

4.1.2 Propellant choice and operations

The **400 N main engine** uses the storable propellants Monomethylhydrazine MMH as fuel and pure Dinitrogen Tetroxide N2O4 or Mixed Oxides of Nitrogen (MON-1, MON-3)

as oxidizer. It is designed for long term steady state operation. It operates in a wide pressure range at regulated pressure mode. The combustion chamber and a part of the nozzle are made of platinum alloy. This solutions does not require surface coating, thereby allowing operational wall temperatures up to 1.600°C (2.900°F) and thus maximum engine performance. The engine can be provided with supporting structure and thermal shield as completely assembled module on customer request.
The **10N bipropellant thruster** is a small rocket engine that uses the storable propellants monomethylhydrazine MMH as fuel and pure di-nitrogen-tetroxide N2O4, or mixed oxides of nitrogen (MON-1, MON-3) as oxidizer. It is designed for both, long term steady state and pulse mode operation. It operates in a wide pressure range at regulated pressure as well as in system blow down mode with flight heritage down to 6 bar inlet condition. Combustion chamber and nozzle are made of platinum alloy that does not need any surface coating. It allows operational temperatures up to 1.500°C (2700°F) and thus maximum thruster performance. The uncoated surface is absolutely resistant against oxidization and thus is invulnerable to mishandling, micrometeoroid impact as well as to application of test sensors and to millions of pulse cycles. Trimming orifices between valve and injector provide for individual adjustment of the propellant flow according to the designed system pressure. Two types of propellant flow control valves may be applied: single seat or dual seat equipped with torque or linear motors.
The choices of the architecture and the propellant rely on these fundamental aspects:

- Liquid propulsion allows re-ignition, variable and controllable thrust
- The propellant couple guarantees high specific impulse and high energy density content
- The propellant is characterised by long lifetime due to high chemical stability
- The pressure fed system is lighter with respect to other solutions and it can be used for smaller and more precise manoeuvres

Propulsion subsytem

Architecture	Bi-Propellant pressure fed system
Fuel	Monomethylhydrazine (MMH)
Oxidizer	Dinitrogen Tetroxide (N2O4)
Propellant tanks volume	$2 \times 270\,\mathrm{L} = 540\,\mathrm{L}$
Propellant mass	$458.4[kg]$

Table 4.2: Data from ESA (2022b).

Main engine

Quantity	Value
Thrust range	$340 - 450[N]$
O/F	$1.6[-]$
Specific impulse	$321[s]$
Mass of the thruster and valve	$4.3[kg]$
Launch mass	1223

Table 4.3: Data from satsearch.co

4.2 Propulsion subsystem sizing

This section is focused on the propulsion subsystem sizing process starting from the ΔV_{budget} obtained starting from the manoeuvres in the Mission Analysis. The sizing is done according to the ESA (2022a) document.

$$\Delta V_{budget} = 1.373\,\text{km/s} \tag{4.1}$$

Propulsion subsystem data

Quantity	Value
Specific impulse	$321[s]$
Nominal dry mass at launch	$640.7[kg]$

Table 4.4: Data from ESA (2022b)

Following the margin *MAR-MAS-040* from the ESA document cited before, *total dry mass at launch of the spacecraft shall include a 20% system level margin of the nominal dry mass at launch*

$$m_{TOTdryatlaunch} = 1.2 m_{nominaldrymassatlaunch} = 768.8\,\text{kg} \tag{4.2}$$

Applying *MAR-DV-010*, the ΔV_{budget} is incremented of 5%:

$$\Delta V_{budget} = 1.44\,\text{km/s} \tag{4.3}$$

In this preliminary sizing the Tsiolkovsky rocket equation is used:

$$\frac{M_0}{M_f} = e^{\frac{\Delta V}{I_{sp} g_0}} = 1.58 \tag{4.4}$$

Where M_0 is the total mass of the s/c and M_f is the final mass of the s/c.

$$M_0 = 1214.8\,\text{kg} \tag{4.5}$$

$$M_{prop} = 446\,\text{kg} \tag{4.6}$$

The obtained propellant ass is incremented of 2% due to *MAR-MAS-080*

$$M_{prop,real} = 457.12\,\text{kg} \tag{4.7}$$

This quantity takes into account the propellant mass required for the main manoeuvres of MEX, so we include the mass allocated for the attitude control manoeuvres($14.2kg$), taken from ESA (2022b). In this way we got the total propellant mass of the spacecraft:

$$M_{prop,tot} = 471.32\,\text{kg} \tag{4.8}$$

The system consists of a liquid bi-propellant architecture, with the properties shown in Tab. 4.5. Considering the *MAR-CP-010* margin for the volume of the tanks:

$$V_{fu,tank,real} = 1.1 V_{fu} = 0.227\,\text{m}^3 \tag{4.9}$$

$$V_{ox,tank,real} = 1.1 V_{ox} = 0.222\,\text{m}^3 \tag{4.10}$$

Pressure values

Quantity	Value
P_{cc}	$10.35[bar]$
$\Delta\ P_{inj}$	$3.11[bar]$
$\Delta\ P_{feed}$	$0.5[bar]$

Quantity	Value
Fuel density$[kg/m^3]$	880
Oxidizer density $[kg/m^3]$	1440
Fuel mass	$m_f = \frac{m_{prop}}{1+OF} = 181.28kg$
Oxidizer mass	$290.04kg$
Fuel volume	$V_{fu} = \frac{m_{fu}}{\rho_{fu}} = 0.206m^3$
Oxidizer volume	$V_{ox} = \frac{m_{ox}}{\rho_{ox}} = 0.201m^3$
Tanks height	$h = 0.6m$

Table 4.5

Titanium Ti6A14V

Quantity	Value
Density	$2780[kg/m^3]$
σ	$950[MPa]$

Table 4.6: Data from A. Brandonisio, M. Lavagna SSEO-ExerciseSession-PS

It is possible to size the tanks considering titanium tanks with the properties in Tab. 4.6. The pressure inside the tanks is computed starting from the pressure inside the combustion chamber (10.35 bar, data from *satsearch.co*) and considering all the losses:

$$p_{tanks,ox,fu} = P_{cc} + \Delta P_{inj} + \Delta P_{feed} = 13.96bar \tag{4.11}$$

with the values shown in Table above. The tanks are supposed to be cylindrical. We can compute the radius and the thickness:

$$r_{fu} = \sqrt{\frac{V_{fu}}{\pi h}} = 0.347m \tag{4.12}$$

$$r_{ox} = \sqrt{\frac{V_{ox}}{\pi h}} = 0.343m \tag{4.13}$$

$$t_{fu} = \frac{P_{tank} r_{fu}}{\sigma} = 0.510mm \tag{4.14}$$

$$t_{ox} = \frac{P_{tank} r_{ox}}{\sigma} = 0.504mm \tag{4.15}$$

Since the thicknesses obtained represent the minimum thickness that is compliant with the pressure values, from a constructive point of view we choose the thicknesses equal to 1 millimeter. Knowing the radius and the thicknesses of the tanks it is possible to compute the needed volume and mass of Titanium.

$$V_{fu,tank} = 0.001306m^3 \tag{4.16}$$

$$V_{ox,tank} = 0.001291m^3 \tag{4.17}$$

$$V_{prop} = V_{ox,tank} + V_{fu,tank} = 0.0026m^3 \tag{4.18}$$

$$m_{fu,tank} = 3.63kg \tag{4.19}$$

$$m_{ox,tank} = 3.59kg \tag{4.20}$$

We can evaluate the pressurant mass, which is Helium, considering a temperature of $T_{tank} = 298K$ and $P_{press,f} = P_tank = 13.96bar$, $P_{press,i} = 10P_{press,f} = 130.96bar$

$$m_{press} = \frac{P_{tank}V_{prop}}{R_{Helium}T_{tank}} \frac{\gamma}{1 - \frac{P_{press,f}}{P_{press,i}}} = 1.57kg \tag{4.21}$$

Pressurant tank can be sized, considering an Helium density of $\rho = 42.56kg/m^3$ at T_{tank} and $130.96bar$ and a spherical tank.

$$r_{tank,press} = (\frac{3V}{4\pi})^{1/3} = 0.475m \tag{4.22}$$

$$t_{tank,press} = \frac{P_{press,ir}}{2\sigma} = 2.75mm \tag{4.23}$$

$$V_{tank,pressurant} = 0.007752m^3 \tag{4.24}$$

$$m_{tank,pressurant} = 21.55kg \tag{4.25}$$

Comparing the results obtained with the real data get from ESA (2022b) :

Comparison with real data

Property	Estimated	Real
Propellant mass[kg]	471.32	476
Fuel tank volume [m^3]	0.227	0.267
Oxidizer tank volume [m^3]	0.222	0.267
Pressurant tank volume [m^3]	0.036	0.035
Fuel tank mass[kg]	3.63	N/A
Oxidizer tank mass[kg]	3.59	N/A
Pressurant tank mass[kg]	21.55	N/A

Table 4.7: Data from ESA (2022b)

4.3 Propulsion subsystem requirements

The propulsion subsystem is a fundamental part of the mission. All the maneuvers designed in the mission analysis must be performed perfectly, eventual failures must be avoided, and its end-of-life passivation must be designed accurately.

The general requirements for the propulsion subsystem are the capability to perform all maneuvers while maintaining a high performance and a low cost and total mass.

More specific requirements and the adopted solution are:

- Redundancy on normally closed pyrotechnic valves (NCPV) shall be applied. It is important because it assures the correct firing of the engine even in case of a valve malfunction. Achieved using an in-parallel configuration in the system. (“The Venus Express Spacecraft System Design” n.d.).

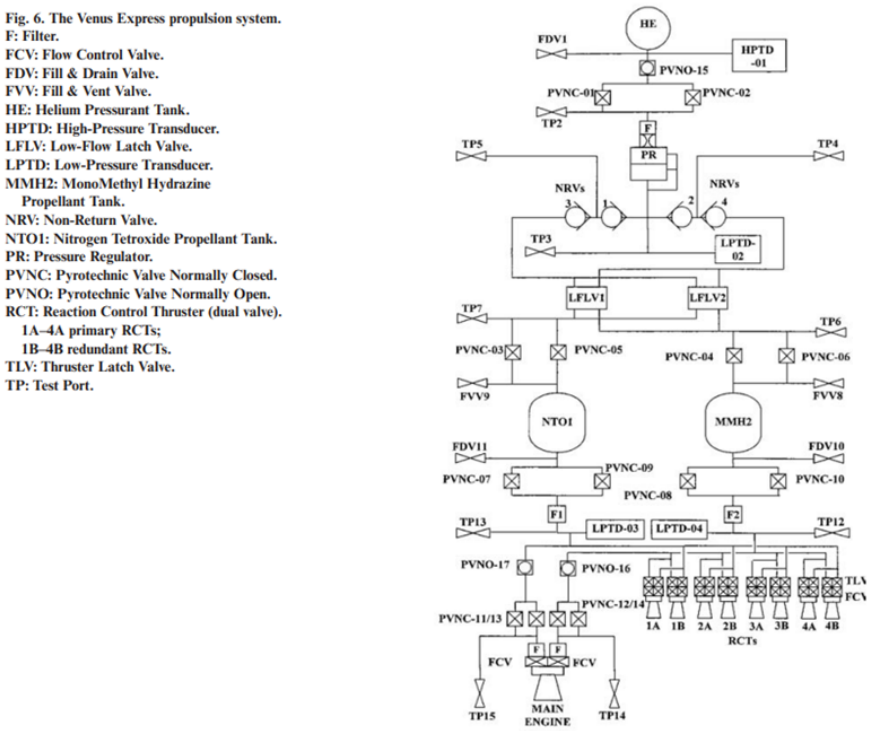

Figure 4.1: Mars Express propulsion subsystem schematics, from "The Venus Express Spacecraft System Design" n.d.

- Shall maintain the propellants above the freezing point, for Hydrazine is around 0°C. Achieved using electric heaters. ("The Venus Express Spacecraft System Design" n.d.).
- Shall maintain a simple, cheap, and reliable design, to address the drivers of the mission. Achieved basing the design on the Eurostar propulsion subsystem, particularly the high-pressure side was very similar. This meant using flight-proven hardware, less testing and reuse of software and numerical models. ("The Venus Express Spacecraft System Design" n.d.).
- Shall prevent the propellant vapor migration upstream during the long coast phase. In microgravity, the diffusion of the propellant upstream can cause damage, specially using a corrosive propellant as hydrazine. Achieved using non return valves (NRV) and flow latch valves to close the line. ("The Venus Express Spacecraft System Design" n.d.).
- Address the launcher requirement to have at least 2 inhibitors between the combustion chamber and the supply, imposed by the Soyuz rules. Achieved using a set of two NCPV in parallel. ("The Venus Express Spacecraft System Design" n.d.).
- Should isolate the engine after the final firing and venting to avoid unnecessary contact between the valves and the propellants. Achieved using normally open pyrotechnic valves. Since this was not a stringent requirement a redundant configuration was not included as it was deemed unnecessary. ("The Venus Express Spacecraft System Design" n.d.).
- Shall accommodate unknown engine thrust imbalances. The calibration date shall be a compromise between two requirements: It should be performed as early as possible to calibrate all maneuvers needed, but as late as possible to avoid excessively prolonged contact between the valves and the propellant. ("The Venus Express

Spacecraft System Design" n.d.). Achieved calibrating the engine after launch.
- Shall allow the propellant to be loaded easily. Achieved using fill and vent and fill and drain valves before and after each tank.
- Shall provide the chosen engine with the correct flow of propellant and power, specifically, the engine (ArianeGroup, n.d.) required:
  - 35W of power at 21 to 27 Volts.
  - 12.5 to 18.5 bar of pressure of propellant
  - 110 to 142 g/s of mass flow rate of propellant.

4.4 Propulsion subsystem design effect

The body of the orbiter is built around the main propulsion system:the two tanks of propellant are one of the most massive and voluminous elements carried on. In order to get the system more symmetric as possible it is convenient put the 2 tanks in a symmetric way. Another important aspect is that putting the fuel tanks in the central part of the orbiter the inertia of the spacecraft is reduced. Moreover, it should be considered that during the mission the fuel is consumed, and so there is a progressive reduction of the total mass and an excursion of the centre of mass and a change in the inertia matrix. The propulsion tanks position near the spacecraft's centre of mass avoids large shifting of the centre of mass itself as the propellant is consumed. These consideration lead to an easier implementation of the ADCS subsystem.

The main engine is aligned to thrust through the centre of mass, whereas engines for attitude control thrust are mounted as far away from the centre of mass as possible to increase the lever arm and thus increase the torque per unit thrust. Misalignments in the centre of gravity due to necessary manufacturing tolerances and thrusters position will show up during thrusting only. This affect most the ADCS that should be able to counteract the disturbance torque generated.

Propulsion lines and tanks must be protected from freezing, usually by thermostatically controlled guard heaters. Power for these heaters should be included in the thermal subsystem. This solution can impose and increment of the overall mass and power demand.

The position of the thrusters affects the location of the scientific payload because the plume can contaminate sensitive surfaces in two main ways:

- Thermal constrains: instrument should be stay away from thrusters to ensure the correct temperature levels
- Operational constrains: Instruments should be aligned with the launch direction to ensure compatibility with thruster plume impingement

Attitude and orbital control subsystem 5

5.1 Mission Phases and Modes

The most relevant mission phases and pointing budget are reported below:

5.1.1 Acquisition Phase

The scope of this mode is to acquire pointing of the Sun and Earth. It is also used during the safe mode, with the Sun acquisition and successively the Earth acquisition to guarantee a power supply and TM/TC link. The accuracy requested is about 0.1° P. Reginer, n.d. to support high-gain antenna communications.

This acquisition requires a star tracker (STR) and Earth/Sun ephemerides. The slew maneuver is calculated to keep the solar panel pointing at the sun and is based on thrusters, once acquisition is complete, finer adjustments are made using the reaction wheels. It is performed mainly in safe mode and after separation from the launcher upper stage.

5.1.2 Nominal Mode

Operational mode in which all scientific observations are made, divided in different phases:

- Wheel damping phase: entry point to normal mode, dynamic transients are settled, the commanded attitude (from ground) is constant.
- Slew phase: enables the satellite a fast slew between two attitudes.
- Fine pointing phase: dedicated to scientific operations.
- Ephemerides pointing phase: the attitude of the spacecraft is defined as a function of the ephemerides of Sun/moon.

The requested pointing is about 0.05° P. Reginer, n.d. during the normal mode, it is performed using the reaction wheels to achieve a higher precision and not to interfere with the instrumentation with the exhaust gas.

5.1.3 Autonomous Wheel Off-loading

The purpose of this maneuver is to prevent wheels from saturation, it is performed using small thruster impulses and is automatic. It activates as soon as one of the wheels speeds is outside the maximum allowed range, it can also be activated or deactivated from ground to avoid interference with important phases.

5.1.4 Main Engine Boost Mode

The purpose of this mode is to achieve and maintain a correct attitude during the engine burns, modified by eventual misalignment of the thrust with respect to the centre of mass. It is performed using the thrusters, the reaction wheels are turned off to avoid interferences in this delicate mode. The attitude is measured using the gyroscopes for a very accurate and short-term attitude measure.

5.2 Configuration

We can divide the different components of the ADCS subsystem into sensors and actuators:

5.2.1 Sensors

To achieve the required pointing accuracy, the spacecraft is equipped with the following sensors:

- **Star trackers:** Used to obtain final 3-axis pointing and in the nominal mode. Is sensible to a magnitude of 5.5, with a medium field of view of 16.4 circular degrees. Two of these units were installed for redundancy, with a 30° between their optical axes. *MEX Instrument overview* n.d.
- **Inertial measurements units:** Two Inertial Measurement Units (IMU), each including a set of 3 gyros and 3 accelerometers were installed. The Gyros were used during the attitude acquisition phase for the rate control, during the observation phase to ensure the required pointing performances and during the trajectory corrections, to achieve a more robust control. To avoid failures, a non-mechanical technology was adopted. The Accelerometers were essential during the main trajectory corrections such as the insertion manoeuvre to improve the accuracy of the delta V. *MEX Instrument overview* n.d.
- **Sun acquisition sensors:** Used in Sun acquisition mode, attitude acquisition or during safe mode, two redundant Sun Acquisition Sensors units (SAS) were installed.

5.2.2 Actuators

The actuators installed on the spacecraft are:

- **Reaction wheel assembly:** Composed by 4 reaction wheels in a skewed configuration, were used to perform all nominal operations using just 3 of them, the fourth one was kept for redundancy. With a request from ground, a 4-wheel configuration can be used to perform critical phases such as before lander ejection or before capture maneuver. The wheels were ball bearing momentum reaction wheels with a maximum torque of 0.075 Nm and a maximum momentum storage of 12 Nms.
- **Attitude thrusters:** Eight 10N thrusters were installed at the corners near the main engine. They were used to balance the thrust misalignment during the main engine boost mode (continuous thrust) and to desaturate the wheels (pulsating mode). The number was doubled for redundancy and in case the misalignment was too high. Since the overall thrust of all 8 engines is similar to the thrust of the

main engine, they can also be used to perform small orbital maneuvers with more precision as they can achieve lower thrust.

5.3 ADCS subsystem design

5.3.1 power demand

The subsystem power demand was estimated adding the assumed power consumption

The estimated power demand is:

Comparison with real data

Instrument	Power consumption [W]	Source
Star tracker	11	(Sodern, n.d.)
Reaction Wheels	20	(Collins, n.d.)
IMU	2	(Estimated)
Thruster valves	8.2	(ArianeGroup, n.d.)

- Total: 77W if the spacecraft uses the sensors and 3 reaction wheels
- Total: 24W if the spacecraft uses just the thrusters.

These results are lower than the real ones, between 115.5 and 65.9 W (Taken from Venus express mission, that had the same ADCS system hardware, under the hypothesys of similar values (Astrium, n.d.)), partly because the power demand of the ADCS computer was not included and partly due to the higher disturbances present in Venus's orbit than in Mars orbit.

5.3.2 Disturbances

An approximate estimation of the maximum disturbances was carried out, the results were:

- **Gravity gradient:** Assuming the inertia moment $I_x = 902\ kg\,m^2$, $I_y = 230\ kg\,m^2$, $I_z = 931\ kg\,m^2$ (from: "Robust FDI applied to thruster faults of a satellite system" n.d.). And the formulas: $T_{gx} = \frac{3\mu}{(2R^3_{orbit})}|I_z - I_y|sin(2\theta)$,
  $T_{gy} = \frac{3\mu}{(2R^3)}|I_z - I_x|sin(2\theta)$, where μ is Mars Planetary constant, R is the radius of the orbit and θ is the angle between the principal axis and the Nadir direction. A maximum torque of $T_{gx} = 1.109\times10^{-3}$Nm and $T_{gy} = 1.9355\times10^{-6}$Nm for non-nadir pointing $sin(2\theta) = 1$ was estimated.
- **Aerodynamic drag:** The value obtained was very low and thus considered negligible, due to the very low atmospheric density of Mars, even at pericentre altitude.
- **Solar radiation pressure:** Assuming as a distance from pressure centre and centre of gravity 0.10m, a solar pressure of $2 \times 10^{-6}N/m^2$, an area of $14m^2$ and q=0.5, using the formula: $T_s = (Cps - Cg)(1 + q)A_{ill} = 4.2 \times 10^{-6}Nm$
- **Magnetic torque:** Assuming a large magnetic dipole moment of D= [0.1 0.1 0.1] J/T, $B = \frac{(2B_0R_0)}{R^3_{orbit}}$, where $B_0 = 5 \times 10^{-8}T$, the magnetic torque is $T_m = D\,B = 2.36 \times 10^{-12}Nm$

- **Main engine misalignment:** A disturbing moment of 10 Nm was assumed during the thrust of the main engine, of the duration of 2000s (P. Reginer, n.d.). The real value, from sources, resulted to be [0.7 5.2 0.0] Nm (M. Lauer, n.d.)

5.3.3 Propellant budget

The propellant budget was calculated considering the contribution of the secular significant torques, calculated as the gravitational gradient for nadir pointing (where $\theta = 0.05°$ is the inclination between the principal axis of inertia and the nadir direction), with a duration of 20 years summed to the estimated torque due to engine misalignment multiplied by the duration of the manoeuvre, this resulted in $H = 2.3471 \times 10^4 Nms$, divided by the specific impulse of 292s, the distance L of 1.15m from the CoM "Robust FDI applied to thruster faults of a satellite system" n.d., g0 and assuming a margin of 100%, this resulted in: $m_{prop} = \frac{H}{(LI_s g_0)} = 14.2kg$.
The real ADCS budget resulted to be 17.6 kg (Astrium, n.d.). The discrepancy is probably due to the lack of real data in our computation.

5.3.4 Reaction wheel design

To design the reaction wheel required momentum a drastic slew manoeuvre of 180° was assumed to be performed in 10 minutes. From the formula derived from (Lavagna, n.d.(a)) the momentum resulted: $M_{wheel} = 4 \cdot \theta_m \cdot \frac{I_{sc}}{t_m^2} = \frac{4 \cdot 180 \cdot \frac{\pi}{180} \cdot I_z}{(60 \cdot 10)^2} = 0.0325Nm$ This result is significantly lower than the real (0.075Nm), but in the same order of magnitude, this discrepancy was attributed to the initial assumptions.

5.4 ADCS requirements

The ADCS which has been developed has to face different environmental conditions. For example, variable distance from the Sun or variable perturbation levels, also the subsystem has to provide numerous pointing facilities, to achieve that, it has to be coordinated with the rest of the system design respecting different requirements and constraints:

Performance requirements:

- **Pointing performance:** during the observation phase and the lander ejection shall be not grater than 0.05°. Also, pointing performance concerning the antenna in order to ensure the earth/satellite link shall be not grater than 0.15°
- **The accuracy of delta-V:** The measured velocities during control manoeuvres shall not be grater than 1% of the true value.

Dynamic constraints:

- **Lander ejection:** Must be performed in a wheel-controlled mode so as not to generate orbit disturbances through the attitude control, before and after the ejection.
- **Sloshing effects:** They are produced by the propellant and can induce sensitive mass and inertia variations during the mission. The system shall mitigate the effects before any manoeuvre

Autonomy constraints:

- **Satellite ground link:** Is a strong constraint, the satellite must ensure an autonomous Earth acquisition and the safe mode must support the communication link.
- **Safe mode:** The satellite should be able to survive without ground contact, caling for safe mode and this minimizes propellant consumption.

TMT&TC subsystem 6

This chapter will present necessary requirements for Telemetry, Tracking, and Telecommunications (TMT&TC) subsystem in order for the MEX mission can achieve its objectives, the preliminary sizing of the subsystem, and a brief discussion about design choices and trade-offs.

6.1 TMT&TC overview

The MEX orbiter can receive and transmit radio signals using two dedicated antenna systems:

- A single High Gain Antenna (HGA), which is a fixed parabolic dish with a diameter of 1.6 m, antenna gain of 40 dBi at X-band and 28 dBi at S-band.
- Two low gain antennas (LGA) with a front and rear placement.

The subsystem is comprised of a duel redundant transponder set up where each unit contains an S- and X-band receiver and transmitter. The X-band is amplified by a traveling wave tube amplifier (TWTA) to a RF power output of 65 W and the S-band downlink by a Solid State Amplifier of 5 W. The HGA is primarily used for receiving telecommands and transmitting high rate telemetry in the operational phase. The LGAs are used during commissioning and emergencies. The following table shows the carrier frequencies:

	Uplink	Downlink
S-band	2.1 GHz	2.3 GHz
X-band	7.1 GHz	8.4 GHz

Table 6.1: Carrier frequencies. (ESA, 2001)

6.1.1 Ground segment

The ground stations used for this mission is the tracking complexes in Perth, Australia, which is a ESA 35 m dish, and NASA's Deep Space Network in California, Spain, and Australia, which uses 34 m and 70 m dishes. The primary ground station is the one located in Perth with its 35 m. A tracking pass usually has a 8 h - 10 h duration and the occurs once a day.

6.2 TMT&TC requirements

This mission main objective is to gain a lot of new information and data from Mars, therefor the orbiter and Earth must be in communication. From the previous section we

know that the orbiter and ground station will be in contact once a day for 8 h - 10 h at a time. Therefore we shall use NASAs Deep Space Network (DSN) or ESAs Deep Space Stations as our ground stations. We know that the mission uses ESAs ground station in Perth as main station. Due to selected ground stations MEX shall use S- and X-band for communication and ,with daily communication, the maximum signal distance between the orbiter and Earth is 2.5 AU, the subsystem must be able to operate at this distance and these RF bands. Due to the high science potential for this mission redundancy is required but redundancy is constrained by mass.

The required data transmission rate will be based on the data outputs from Table 1.7 and Denis et al. (2008). Due to the missing information regarding the exact data output from ASPERA-3 in Table 1.7, an assumption has been made. In Denis et al. (2008, p. 9) ASPERA-3 is classified as a low rate instrument along with PFS, MARSIS, and SPICAM, which generates less than 80 kbps. Therefor assuming ASPERA-3 generates a maximum of 285 Mbit day^{-1}, the same as MARSIS, would insure the link budget is capable of handling the necessary data loads. The orbiter will also generate telemetry data, according to Denis et al. (2008, p. 14) the payload and platform generates 1.1 kbps of "housekeeping" data, which amounts to 95 Mbit day^{-1}. This totals to a daily estimated data size of 2595 Mbit day^{-1} and with a minimum tracking phase of 8 h would require the TMT&TC s/s to downlink 90 kbit s^{-1}.

Due to the distance between MEX and the Earth a narrow beam (high gain) antenna is required for science return, for commissioning and emergency modes omni-directional antennas are required.

Data quality is also of high importance for this mission therefor the TMT&TC s/s must be designed to have a bit error rate (BER) of 10^{-5} or lower.

6.3 Link Sizing

This section will present downlink budget from MEX to the ground station on Perth, Australia, using the X-band at the maximum distance of 2.5 AU. The ground station has a minimum required SNR of 17 dB and the antenna dish size is 35 m according to ESA (2001, p. 26). The frequency used for this downlink is 8.4 GHz is shown in Table 6.1.

According to *Space mission engineering : the new SMAD* (2011, p. 623-634) the theoretical best modulation index is when β approaches 90°, but values from 60° to 90° are typically used for normal-mode downlink bit rates to maximize the received data power. QPSK is often used in high data rate communications because of its power efficiency, the same as BPSK but in half the transmitted bandwidth. For this downlink a QPSK uncoded signal is chosen along with a modulation index β of 60°, and a minimum bit-error-rate of 10^{-5} for the downlink data. This gives a minimums bit-energy to noise-spectral-density $(E_b/N_0)_{min} = 9.6$ dB and adding 3 dB. The downlink data rate R is 90 kbit s^{-1}.

After multiple link budget iterations the antenna size D_{tx} of 0.8 m and power input P_{in} of 45 W was selected. The transceiver power P_{tx} is computed using a TWTA with an efficiancy μ_{amp} of 50%. A TWTA was chosen based on the increased efficiency for high

gain applications compared to Solid State Power Amplifiers (SSPAs).

$$P_{tx} = 10\ \log_{10}(\mu_{amp}\, P_{in}) = 43.52\,\text{dB mW} \tag{6.1}$$

The gain for the transceiver and receiving antenna was computed as follows using the gain equation for a parabolic antenna for both cases. D_{ant} is the antenna diameter in meters, and f is the frequency in GHz.

$$G_{ant} = 17.8 + 20\ \log_{10}(D_{ant}) + 20\ \log_{10}(f) \tag{6.2}$$
$$G_{tx} = 34.35\,\text{dBi} \tag{6.3}$$
$$G_{rx} = 67.17\,\text{dBi} \tag{6.4}$$

The half-power beam is computed using the empirical equation for a parabolic antenna, λ is signal wavelength.

$$\Theta_{rx} = 65.3\,\frac{\lambda}{D_{rx}} = 0.065^\circ \tag{6.5}$$

The signal losses are due internal cables losses on the s/c L_c, atmospheric losses L_a, pointing losses L_p, and space losses L_s, they are a function of the distance r between the s/c and Earth and f.

$$L_c = -3\,\text{dB} \tag{6.6}$$
$$L_p = -0.3\,\text{dB} \tag{6.7}$$
$$L_a = -0.5\,\text{dB} \tag{6.8}$$
$$L_s = 92.45 + 20\ \log_{10}(r) + 20\ \log_{10}(f) = -282.39\,\text{dB} \tag{6.9}$$

The value for L_c usually between 1 dB - 3 dB and it assumed be 3 dB to account for worst case scenario. The value for L_p and L_a was taken from ESA (2001, p. 26). L_s was computed using *Space mission engineering : the new SMAD* (2011, Eq (16-22)).

Now it is possible to compute the equivalent isotropic radiated power, $EIRP$, and the power reicieved by the ground station P_{rx}.

$$EIRP = P_{tx} + G_{tx} + L_c = 74.87\,\text{dB mW} \tag{6.10}$$
$$P_{rx} = EIRP + G_{rx} + L_s + L_a + L_p = -141.16\,\text{dB mW} \tag{6.11}$$

Next we can compute the E_b/N_0 for the receiver capability to translate the signal and distinguish it from the noise. To do that the system noise density N_0 for the s/c is computed with an assumed sensor temperature T_s of 250 K, and k is the Boltzman constant.

$$N_0 = 10\ \log_{10}(k\,T_s) = -204.62\,\text{dB} \tag{6.12}$$
$$E_b/N_0 = P_{rx} - N_0 - 10\ \log_{10}(R) = 13.92\,\text{dB} \tag{6.13}$$
$$(E_b/N_0)_{margin} = 1.32\,\text{dB} \tag{6.14}$$

This gives a positive E_b/N_0 margin, which means the signal can be distinguished from the noise and the ground station can translate the received data. This is a tight margin so the transceiver antenna diameter and input power could be increased to improve the margin.

Another way to verify signal strength is to compute the carrier signal-to-noise ratio, SNR_c, using the signal bandwidth. The signal bandwidth B_{dB} in dB can be computed using the $(E_b/N_0)_{min}$ value, from the required minimum BER, and the following equation.

$$(E_b/N_0)_{min} = \frac{2^{\frac{R_{dB}}{B_{dB}}} - 1}{\frac{R_{dB}}{B_{dB}}} \Downarrow \tag{6.15}$$

$$B_{dB} = 7.82\,\text{dB Hz} \tag{6.16}$$

To ensure a proper channel capacity, i.e. $R_{dB} <$ Channel capacity, 3 dB will be added to the current B_{dB}, so $B_{dB} = 10\,\text{dB Hz}$. Increasing the bandwidth equates to the following channel capacity, C_{cap}:

$$R_{dB} = 10\,\log_{10}(R) = 49.5\,\text{dB} \tag{6.17}$$

$$C_{cap} = B_{dB}\,\log_2\left(1 + (E_b/N_0)_{min}\,\frac{R_{dB}}{B_{dB}}\right) = 59.87\,\text{dB} \tag{6.18}$$

This mean that the bandwidth would be sufficient even if the data rate would increase.

We can now compute SNR_c and the SNR margin using the carrier power and modulation loss:

$$P_{mod,loss} = 20\,\log_{10}(\cos(\beta)) = -6.02\,\text{dB} \tag{6.19}$$

$$P_c = P_{rx} + P_{mod-,loss} = -147.18\,\text{dB} \tag{6.20}$$

$$SNR_c = P_c - N_0 - B_{dB} = 47.44\,\text{dB} \tag{6.21}$$

$$SNR_{margin} = SNR_c - SNR_{min} = 30.44\,\text{dB} \tag{6.22}$$

The downlink budget is now complete, with a s/c antenna of 0.8 m and a power input of 45 W the s/c can communicate with Earth.

6.4 TTM&TC subsystem design effects

The choice of the High Gain Antenna frequency affected both the satellite and the ground station transmitter power and moreover the size of the antenna itself. The TTM&TC subsystem is composed of 2 omnidirectional Low Gain Antennas used when attitude control in unknown, located on opposite sides of the orbiter, in order to ensure communication with the earth in every s/c attitude. There are 2 dual-band transponders to ensure dual redundancy to account a single transponder failure. All these aspect cause an increment of the overall mass (meaning also more propellant and higher costs) of the orbiter and its power demand.

Antennas are sensible to the temperature and in particular it increases the noise, so the heating sources (ex: batteries) should be put away from antennas. Antennas require the correct power and voltage to work properly. This means sizing the power subsystem properly to ensure the requested amount of power (Solar arrays and batteries) and the right voltage (Power control and distribution Units).

During communication with the Earth in nominal conditions, the High Gain Antenna shall point toward the Earth with a very precise accuracy. For this reason, the s/c should

be able to slew every time there is the communication windows, and to maintain the right attitude during the whole time. This should be ensured by the AOCS subsystem. Moreover, must make sure the satellite's body or other appendages such as the solar arrays do not obscure the antenna's field of view during transmission, so the solar arrays should be mounted on a different surface with respect to the antenna. Another important aspect is that during transmission no science operation were performed because instruments did not point toward Mars surface. So, for this reason science operation cannot occupy all the Mars orbit, but only a small fraction of that.

Electric Power Subsystem 7

This chapter is focused on the description of the the Electric Power Subsystem (EPS) adopted in Mars Express mission, including the principal design aspects, the analysis of the requirements and a preliminary sizing of the unit.

7.1 Electric Power subsystem overview

Electrical power is provided by the spacecraft's solar panels with an area of 11.42 m^2 and equipped with BSR Silicon cells (Si-BSR 2PR/200, with 100 µm cover glass thickness to cope with Mars radiation environment) which are folded against its body during launch and deploy shortly after the launcher housing has been jettisoned. The panels are mounted on a 1-DOF SADM which tilts them forwards and backwards to catch most sunlight.

When the spacecraft's view of the Sun is obscured during a solar eclipse, 3 identical lithium-ion batteries with a capacity of 22.5 Ah each and with a 6s16p configuration (16 parallel-connected strings of 6 Sony 18650HC cells in series), previously charged up by the solar panels, will take over the power supply.

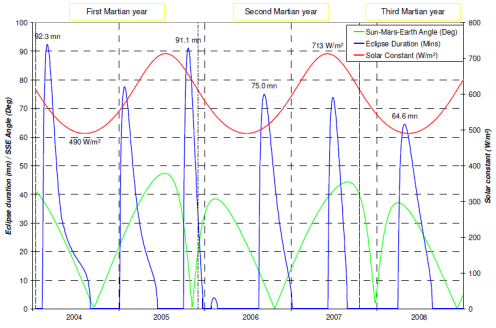

Figure 7.1: MEX orbital events (LOCHE, 2008)

Each battery is connected to a separate battery charge-discharge regulator, controlled such as to ensure equal current sharing between batteries. Ones reaching the final orbit, the orbital period is 6.7 hours (near 11 revolutions in 3 sol (Martian day)). The maximum eclipse duration was about 90 min, at the end of the first Martian year. The number of eclipses and maximum eclipse duration varies from one season to another as can be seen from Figure 7.1.

Regarding the power control unit and the power distribution the Orbiter has a + 28 V ± 1% regulated voltage at the output of the array power regulator. During daytime the batteries are charged through step-down current controlled BCR. A PPT architecture was adopted, so if the Solar Array power exceeds the total spacecraft demand, including battery recharge, main bus regulation is performed by the array power regulator. A separate redundant power regulator and PPT is provided for each of the two Solar Array wings.

The Mars Express power distribution is based on a centralised scheme and it is ensured by the PDU. Each power line is switched and protected by means of a LCL as a protection

device in case of over current. A total of 78 LCL are implemented within the PDU. It is however not possible for all units to isolate the primary voltage for some units in case of overcurrent. For the CDMU and for the Dual Band Transponder Receivers the primary power is distributed to them through FCL, devices identical in essence to LCL, except that they do not feature ON/OFF switching capability. 6 FCL are in the Mars Express PDU. (*SpaceOps 2006 Conference* 2006)

7.2 Power Budget breakdown

From the previous sizing of the propulsion, AOCS, TTM&TC subsystem and the scientific payload it is possible to get an estimation of the power demand that each subsystem requires. Regarding the data handling, thermal and power subsystem, their power budgets are estimated according to the guidelines from *Wiley J. Larson and James R. Wertz, Space Mission Analysis and Design - thrid edition , in 10.3 Design Budjet, the Space Technology Library Ed., California, ISBN 1-881883-10-8, pp. 314-316, 2005.* and the following considerations and hypothesis:

- The operating power of the orbiter is assumed 550W
- C&DH it is assumed to require 6% of the total power budget
- TCS it is assumed to require 5% of the total power budget
- EPS it is assumed to require 10% of the total power budget

With these assumptions the following power budgets (Table 7.1) are obtained:

Subsystem	Power demand
C&DH	33 W
TCS	27.5 W
EPS	55 W

Table 7.1: Estimated power demand

There is the needed to identify the most relevant mission modes in order to obtain their power demand and so to catch the sizing mode in terms of power budget. All these are collected in the Figure 7.3 below. To do that some assumptions were considered:

- Not all the instruments work together. The selection of the instruments working during daylight conditions and eclipses, during low or high altitude it is made accordingly to the Figure 7.2. No operations are performed at high altitude in eclipse condition.
- In the manoeuvre and communication modes no science operations are performed.
- It was supposed that all the instruments are turned on but only some of them or none are working together during each mode. For this reason, the power consumption of each instrument in no-working condition is estimated considering the 15% of its consumption when the instrument works.
- The communication mode is performed only in light conditions.
- In the estimation of the propulsion low thrust power demand, it was considered that 4 engines work together, while only 2 are at least used to provide and maintain the correct altitude, giving a net torque in the other modes.
- In the s/c are mounted 4 reaction wheels but 3 are used and one is for redundancy to improve the reliability of the system: it was considered the power consumption

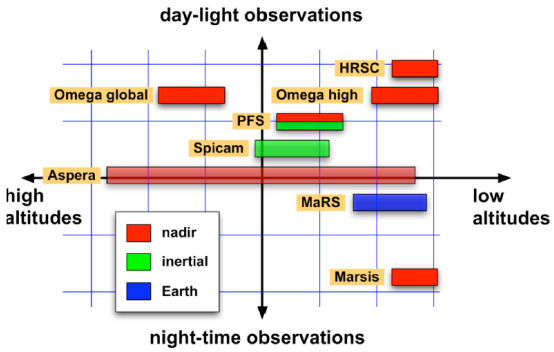

Figure 7.2: Observation requirements of MEX instruments in terms of illumination conditions, altitude, and pointing type (R. Pischel, 2009)

coming from 3 reaction wheels working together in nominal condition. A 4-wheels configuration can be used to perform critical phases such as before lander ejection or before capture maneuver; this was consider in the 'high thrust' manoeuvre mode.

- Some margins were applied in accordance with the ESA standard (ESA, n.d.), in particular:
  - MAR-PWR-020: it was assumed just the 2% of margin because in the power budget breakdown it was considered yet the maximum power demand for each instrument as the worst-case scenario.
  - MAR-PWR-040

The sizing mode for the power storage device is the 'Earth-pointing' operating condition in the eclipse, while the sizing condition for the primary energy source is the communication mode in X-band.

The real average power demands required for the different modes are reported in the Table 1.3: these values are quite similar for what concern the observation modes and a bit different with respect to the other modes, in particular regarding the spacecraft power demand. In general, the obtained values are quite small with respect to the real ones. More precise data on the real power budget breakdown were not found.

SUBSYSTEM	SCIENCE OPERATION					MANOEUVRE		COMMUNICATION	
	DAYLIGHT			ECLIPSE					
	LOW ALTITUDE		HIGH ALTITUDE	LOW ALTITUDE		HIGH THRUST	LOW THRUST	X-band	S-band
	NADIR POINTING	INERTIAL POINTING		NADIR POINTING	EARTH POINTING				
INSTRUMENTS 2% margin	**131.36**	**101.62**	**89.14**	**103.79**	**112.15**	**47.87**	**47.87**	**47.87**	**47.87**
INTRUMENTS	**128.78**	**99.63**	**87.39**	**101.75**	**111.93**	**46.93**	**46.93**	**46.93**	**46.93**
HRSC	48.7	7.31	7.31	7.31	7.31	7.31	7.31	7.31	7.31
OMEGA	47.6	7.14	47.6	7.14	7.14	7.14	7.14	7.14	7.14
ASPERA-3	13.5	13.5	13.5	13.5	13.5	13.5	13.5	13.5	13.5
PFS	6.6	44	6.6	6.6	6.6	6.6	6.6	6.6	6.6
SPICAM	2.7	18	2.7	2.7	2.7	2.7	2.7	2.7	2.7
MARSIS	9.68	9.68	9.68	64.5	9.68	9.68	9.68	9.68	9.68
MaRS	0	0	0	0	65	0	0	0	0
SPACECRAFT	**197.9**	**197.9**	**197.9**	**197.9**	**197.9**	**252.9**	**214.3**	**287.9**	**207.9**
ADCS	**66**	**66**	**66**	**66**	**66**	**86**	**66**	**66**	**66**
RW	60	60	60	60	60	80	60	60	60
STR	2	2	2	2	2	2	2	2	2
IMU	4	4	4	4	4	4	4	4	4
C&DH	**33**	**33**	**33**	**33**	**33**	**33**	**33**	**33**	**33**
EPS	**55**	**55**	**55**	**55**	**55**	**55**	**55**	**55**	**55**
TCS	**27.5**	**27.5**	**27.5**	**27.5**	**27.5**	**27.5**	**27.5**	**27.5**	**27.5**
TTMTC	**0**	**0**	**0**	**0**	**0**	**0**	**0**	**90**	**10**
X-Band RW=65W	0	0	0	0	0	0	0	90	0
S-band RW=5W	0	0	0	0	0	0	0	0	10
PS	**16.4**	**16.4**	**16.4**	**16.4**	**16.4**	**51.4**	**32.80**	**16.4**	**16.4**
main engine (400 N)	0	0	0	0	0	35	0	0	0
ADCS engines (10 N)	16.4	16.4	16.4	16.4	16.4	16.4	32.80	16.4	16.4
TOTAL	***329.3***	***299.5***	***287.0***	***301.7***	***310.1***	***300.8***	***262.2***	***335.8***	***255.8***
TOTAL 20% margin	***395.2***	***359.4***	***334.4***	***362.0***	***372.1***	***361.0***	***314.6***	***403.0***	***307.0***

Figure 7.3: Power budget breakdown

7.3 Primary energy source sizing

By looking at the Figure 7.4 it is possible to observe that considering a nominal duration of the mission of a bit more than 2 years (1 Martian years plus cruise phase) and a load power less than 1 kW, the optimal solution in term of primary power generation is the photovoltaic choice. This confirms the choice adopted on the MEX orbiter. In particular in the following preliminary sizing it was assumed to use silicon cell type, as the real, design with a specific power equal to 25 W/kg, a voltage of 0.5 V each and an area of 40x40 mm^2.

Moreover it was assumed that system nominal voltage is 28 V. Mission life and the average power requirement are the two key design considerations in sizing the solar array for the spacecraft. First it is necessary to determine how much power (P_{sa}) the solar array must provide during daylight to power the spacecraft for the entire orbit accordingly to the following formula:

$$P_{sa} = \frac{P_d T_d}{X_d T_d} + \frac{P_e T_e}{X_e T_d} \tag{7.1}$$

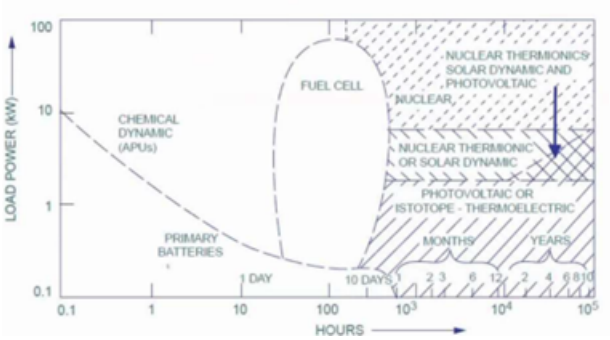

Figure 7.4: Power density with respect to mission lifetime (Lavagna, n.d.[b])

where P_e=372.1 W and P_d=403 W are the sizing power demand in eclipse and sunlight condition respectively while T_e=1.50 h and T_d=5.2 h are the time spent in eclipse or light. The PPT configuration (X_e =0.60 and X_d=0.80) it is assumed in accordance to the real one because it is the optimal choice for medium/large spacecraft in a planetary mission that should perform lots of eclipse/light cycles during its lifetime.

The second step is identify the power source characteristics in order to compute the power generated at BOL and the one at the EOL taking into account the main inefficiency that are:

- Inherent loss: I_d=0.77 (it takes into account all the integration of the system)
- Cosine loss: α=6.68° is the solar aspect angle.(Lavagna, n.d.[a])
- Silicon cell efficiency: η=15%
- Degradation factor: d=2.75% per year (it considers the average degradation of the cells accordingly to their technology)

The solar density power P_0 depends on the distance from the Sun since the solar constant varies from 490 W/m^2 (apocentre) up to 710 W/m^2 (pericentre)(Daniel, n.d.). To perform the sizing, the worst condition is taken into account, that means solar constant equal to 490 W/m^2. A nominal life of the mission equal to 2.42 years (1 Martian year + 6 months of cruise) was considered for the preliminary sizing.

All the obtained results are summarized in Table 7.2:

Results

		Estimated	Real
P_{sa}	[W]	682.64	650
P_0	[W/m^2]	73.5	-
P_{BOL}	[W/m^2]	56.21	-
P_{EOL}	[W/m^2]	52.62	-
A_{sa}	[m^2]	12.992	11.42
Mass	[kg]	27.3	45.9
$N_{cell_{TOT}}$	[-]	8120	-
N_{ser}	[-]	56	-
V_{real}	[V]	28	28

Table 7.2: Solar arrays sizing results

The computed P_{sa} results higher with respect to the real one that nominally is about 650 W due to an over-estimations made in the preliminary sizing process and as consequence

also the solar panel area results quite high with respect to the real one. More in detail, 8120 solar cells are needed in total to cover the required area and it is necessary to put 56 cells in series. From these it is possible to recalculate the real number of cells providing the right power and voltage and so the actual arrays area that in this particular case correspond exactly to the values previously computed. Despite the over-sizing of the solar arrays it results that their mass is almost a half of the real one. One reason can be found in the fact that the real mass value does not include only the mass of the solar cells but also the ones related to the other components of the solar arrays system.

7.4 Secondary energy source sizing

A secondary energy source is needed due to the fact that during the orbit the Orbiter experiences some eclipse conditions and moreover a power storage device is usually required by the Safe Mode. Secondary batteries recharge in sunlight and discharge during eclipse. The required energy assessment deriving from the sizing condition of power in the operational mode P_e =372.1 W and the eclipse time T_e =1.50 h, is E=558.15 Wh. First a preliminary analysis was performed to estimate T_e using the following simple model considering h as the semi-major axis of the orbit:

$$\beta = cos^{-1}(\frac{R_M}{R_M + h}) \tag{7.2}$$

$$T_e = T\frac{180 - 2\beta}{360} \tag{7.3}$$

The resulting T_e turn out to be lower with respect to the real one due to the fact that the model suites for circular orbit while the orbit under study is highly eccentric. For this reason T_e used during the sizing process it is assumed as the maximum real value (90 min).

An important parameter to estimate in order to get the operational profile assessment is the DOD that depends on the number of charge/discharge cycles experienced during the mission life: 3452 cycle are obtained in total and from the Figure 7.5 it is estimated a DOD equal to about 40%.

Following the real design to perform the sizing, 3 lithium-ion batteries with 95% of efficiency were chosen (*SpaceOps 2006 Conference* 2006). Moreover it is supposed to

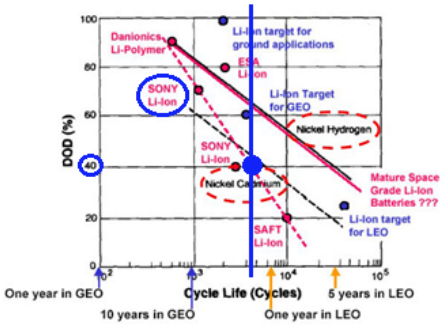

Figure 7.5: DOD with respect to eclipse/sun cycles (Lavagna, n.d.[b])

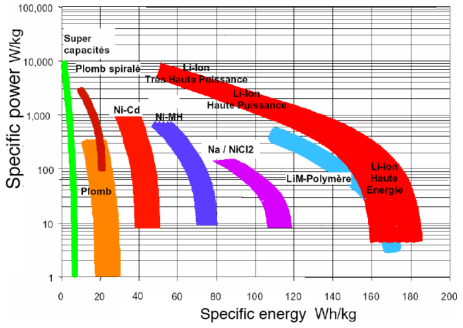

Figure 7.6: Secondary batteries: performance comparison (Lavagna, n.d.[b])

use the same cell with a maximum voltage of 4.2 V, a capacity of 1.5 Ah, E_d equal to 125 Wh/kg and E_v=318 Wh/liter. The choice of assuming the specific energy of the battery quite low with respect to the mean value of Li-ion battery (150 Wh/kg) is related to the Figure 7.6: considering that a more 'high-power' battery can realise high energy in a small amount of time the choice is compliant with the mission profile under study that includes quite short eclipses. The system nominal voltage is set at 28 V.

Starting from these statements it is possible to evaluate the capacity of each battery and its rate of charge. In addition knowing the cell and system voltage it is possible to retrieve the required number of cells in series and as a consequence the number of string, supposing a package efficiency of 80%. The results obtained from the preliminary sizing for each battery are summarized in Table 7.3:

Results

		Estimated	Real
C_r	[Wh]	489.61	630
C_r	[Ah]	17.48	22.5
R	[A]	1.17	-
N_{ser}	[-]	7	6
V_{real}	[V]	29.4	11.42
C_{string}	[Ah]	35.28	-
N_{string}	[-]	14	16
C_{real}	[Ah]	17.64	-
$Mass$	[kg]	3.9	5
$Volume$	[dm^3]	1.54	1.98

Table 7.3: Batteries sizing results

In general, the batteries result undersized with respect to the real system. One possible cause can be related to the fact that in this preliminary sizing it is assumed an average constant DOD with a graphical estimation based on the total number of charge/discharge cycle that the Orbiter performs. In the real situation instead, the DOD evolution in time follows the eclipse profile. In particular the maximum DOD reached is 49% and the average DOD is only 11%. (LOCHE, 2008)

7.5 Electric power subsystem Requirements

The EPS shall supply a continuous source of electrical power to spacecraft loads during the mission life in order to satisfy the mission. More in detail this subsystem shall:

- have a source of power: the solar array must supply enough power for operations and recharging the battery until end-of-life. This means that the EPS shall cope with a highly variable environment: first Earth-Mars distance and then Sun-to-Mars distance that impact on Solar flux. Solar arrays shall be folded during launch, so they shall be deployable and they shall cope with the launch sizing requirement. Moreover, due to their importance for the success of the mission the system shall perform a correct solar arrays deployment in a reliable way.
- have batteries to storage enough power needed during eclipses (and Safe Mode).
- provide the right power (current and voltage) at each loads.

- control and distribute electrical power to the spacecraft.
- support power requirements for average and peak electrical loads.
- provide converters for AC and regulated DC power buses.
- protect the spacecraft payload against failures within the EPS and bus. For this reason it is needed a sufficient redundancy to improve reliability of the system.

7.6 Electric Power subsystem design effects

Energy storage usually means large, heavy batteries and all their characteristics shall be take into account: Battery and PDU are positioned opposite to heavy elements like the transponder for TTM&TC , Marsis instrument to balance the overall mass. They are also located perpendicular to the solar arrays in order to not receive directly the sunlight improving the thermal control. The more reliable adopted systems to charge the battery and deploy the solar arrays increments the overall mass of the system and so the propellant mass and the overall cost.

Solar arrays first of all have an impact on the inertia matrix. They are mounted in a symmetric way on +-y axis as it possible to observe in Figure 9.1 in order to maintain the centre of mass as near as possible to the geometric centre of the s/c. All the instruments and devices that shall not take direct sunlight should be mounted perpendicular to the solar arrays.

Finally the battery should stay between -10 and +15 °C, while electronic components around -10 and +40°C. They affect in a large way the sizing of the thermal subsystem.

Thermal Control subsystem 8

This chapter will present a critical analysis if the thermal control subsystem,the preliminary sizing of the subsystem and the main requirements are discussed.

8.1 Thermal control requirements

The MEX thermal subsystem requirements can be identified as:

- Some parts of the spacecraft must be kept warm and other parts cold to provide the right environments for the science instruments and onboard equipment. The inside of the spacecraft **shall** be maintained 10°-20° Celsius (50°-68° Fahrenheit) by covering it with thermal blankets made from gold-plated aluminum-tin alloy.
- Most of the instruments **shall** be kept at room temperature (10°-20° Celsius or 50°-68° Fahrenheit), but two instruments (PFS and OMEGA) have infrared detectors that **shall** be kept at very low temperatures (about -180° Celsius or -292° Fahrenheit). Radiators for these instruments release excess heat into space, which is very cold (about -270° Celsius or -454 Fahrenheit). The sensors on the camera (HRSC) also need to be kept cool.
- Material not covered by insulation such as the solar array and the high-gain antenna may face temperatures of -100° Celsius (-148° Fahrenheit) in the shade and up to 150° Celsius (302° Fahrenheit) in sunlight. To keep these parts from shrinking and expanding in such temperature variations, they are made of composite materials that can withstand wide temperature variations, as it would require too much power to keep them at room temperature.
- The thermal system shall prevent the feeding lines from freezing: Oxidizer Freezing Point: $-11°C$, Fuel Freezing Point: $-52°C$.
- Maintaining an optimal thermal environment is the task of the craft's thermal subsystem. The thermal subsystem includes electrical heaters where needed to keep the spacecraft warm (e.g. to prevent fuel lines from freezing) and passive radiators to keep other units cool. In this way Mars Express can perform scientific observations.

8.2 Thermal subsystem design effect

As well as keeping MEX warm, it is important to know how much power is needed to achieve this. Power is supplied by either the solar arrays (when exposed to sunlight) by the batteries during an eclipse. Power produced by either the solar arrays or batteries is used for platform operations, thermal operations and whatever remains is available for science. The energy provided by the batteries during an eclipse is finite, so knowing how

much power is needed for the thermal subsystems means mission controllers can know how much power is available for science. Knowing accurately how much power is needed by the thermal subsystem means we can really maximise science observations. Computing the power needed by MEX is really complex, since it depends on:

- **Sun distance.** The Sun emits solar flux, measured in W/m2, (power per square meter received) and the further away from the Sun, the less flux received – and so the cooler is Mars Express.
- **Solar angle.** This is the angle of the spacecraft with respect to the Sun. Where is the Sun is shining on MEX. On the top (+Z face), the bottom (-Z face) or the +X face, and at what angle to that face. This will affect the craft's temperature.
- **Distance from Mars.** The albedo is the amount of energy reflected off the planet. 'Mars shine' refers to the amount of energy being reflected by the planet and can affect MEX's thermal condition.
- **Mars-Sun distance.** This affects the Mars albedo, which in turn affects MEX.
- **Eclipses.** As seen above, during eclipse, MEX is in Mars' shadow, receiving no illumination from the Sun, and this can cause a dramatic cool down.
- **Operations on going on the spacecraft.** Certain operations, such as using the transmitter to communicate with Earth, warm up certain sections of the spacecraft.

8.3 Thermal control sizing

To size the thermal control systems we need to have operating temperatures that are necessary for the spacecraft to operate nominally. The operating temperature range mention in the requirements section (10 °C - 20 °C ±15 °C) will be used for the hot and cold case calculations. To further define the variables necessary, first, the equations for each case need to be understood. For the hot case, there are multiple variables that affect the thermal gradient within a spacecraft. The variables are the following: internal heat generated (Q_{int}), radiation of sun on s/c (Q_{sun-sc}), albedo of a nearby planet (Q_{alb}), infrared radiation of a nearby planet (Q_{ir}), and the emitted heat of the s/c (Q_{emi}). Put together in Eq (8.1).

$$Q_{int} + Q_{sun-sc} + Q_{alb} + Q_{IR} - Q_{emi} = 0 \tag{8.1}$$

$$Q_{emi} = \varepsilon \, \sigma \, A_e T_{sc}^4 \tag{8.2}$$

To find the temperature of the s/c a substitution of the equation of the flux emitted by the s/c (Eq. (8.2)) is inserted and a manipulation of the variables in equation (8.1) leaves the temperature of the s/c as the single variable. This is demonstrated in Eq (8.3).

$$T_{sc} = \sqrt[4]{(Q_{int} + Q_{sun-sc} + Q_{alb} + Q_{IR})/(\varepsilon \, \sigma \, A_e)} \tag{8.3}$$

Table 8.1 shows the results of every flux value needed to calculate the temperature of the s/c in the hot case. An in-depth break down of the equations for every variable is shown below:

Description	Unit	Value
Q_{int}	[W]	500
q_o	[W/m^2]	607.778
Q_{sun-sc}	[W]	121.601
Q_{alb}	[W]	25.658
Q_{IR}	[W]	706.318
ε	[-]	0.7
σ	[W m^{-2} K^{-4}]	5.67×10^8
A_e	[m^2]	14.64
R_{sc}	[AU]	2.25

Table 8.1: Hot Case values

$$q_{sun-sc} = q_o \, R_{sc}^2 \tag{8.4}$$

Here Eq (8.4) is the flux generated by the sun and received by the s/c per m^2.

$$Q_{sun-sc} = A_{sun} \, \alpha \, \cos(\nu_{sun}) \, q_{sun-sc} \tag{8.5}$$

Eq. (8.5) is the total heat flux reaching the spacecraft from the sun.

$$Q_{alb} = A_{pl} \, \alpha \, cos(\nu_{pl}) \, q_{sun-sc} \, a \, (R_{pl}/R_{orbit})^2 \tag{8.6}$$

Eq. (8.6) is the total heat flux reaching the s/c from the albedo of mars.

$$Q_{IR} = A_{pl} \, cos(\nu_{pl}) \, \sigma \, \varepsilon \, T_{pl}^4 \, (R_{pl}/R_{orbit})^2 \tag{8.7}$$

Eq (8.7) is the total flux reaching the spacecraft from the infrared radiation of mars.

$$Q_{int} = (1 - \varepsilon_{SA}) \, A_{SA} \, q_{sun-sc} \tag{8.8}$$

Eq. (8.8) is the total heat flux generated inside the s/c

The final temperature of the s/c in the hot case is 296.85 K or 23.7 °C which falls between the necessary range mentioned in the requirements.

In the cold case, there are much less variables to deal with so the calculations are simple and still use some of the values calculated previously. The variables needed to calculate temperature in the cold case are: (Q_{ir}), which continues to be the heat flux coming from the infrared radiation off the nearby planet to the s/c. (Q_{int}), which differs from the hot case because during eclipses since less of the components are operating and therefore less heat is generated. (Q_{emi}), is used in the hot case to determine the temperature of the s/c.

This table represents the values needed to calculate the final temperature of the s/c in the cold case. Notice that the internal heat generated by the s/c is different then in the hot case.

$$Q_{int} + Q_{IR} - Q_{emi} = 0 \tag{8.9}$$

Description	Unit	Value
Q_{int}	[W]	360
Q_{IR}	[W]	706.318

Table 8.2: Cold Case values

$$Tsc = \sqrt[4]{(Q_{int} + Q_{IR})/(\varepsilon\,\sigma\,A_e)} \tag{8.10}$$

The final temperature of the s/c in the cold case is 279.66 K or 6.51 °C which falls between the necessary range mentioned in the requirements.

Structure and configuration 9

This chapter presents and critically analyzes the overall configuration and structure of the spacecraft.

The spacecraft configuration is relatively simple, the design is optimized for a Soyuz-Fregat launcher but is also compatible with a Delta II vehicle.

The load paths are basic and payload interfaces are standardized to enable a cheap, simplified, and low risk development.

The design is based on a parallelepipedal shape about 1.7m length, 1.7m width and 1.4m height. To minimize the dry mass of the spacecraft and to offer large mounting surfaces and volumes, compatible with different instruments for future missions, the traditional cylindrical core structure was deemed less efficient than a stiffened box configuration, with a cylindrical launcher adapter at the bottom. This structure limits the number of complex elements. The solar arrays are symmetrical to minimize aerodynamic torques.

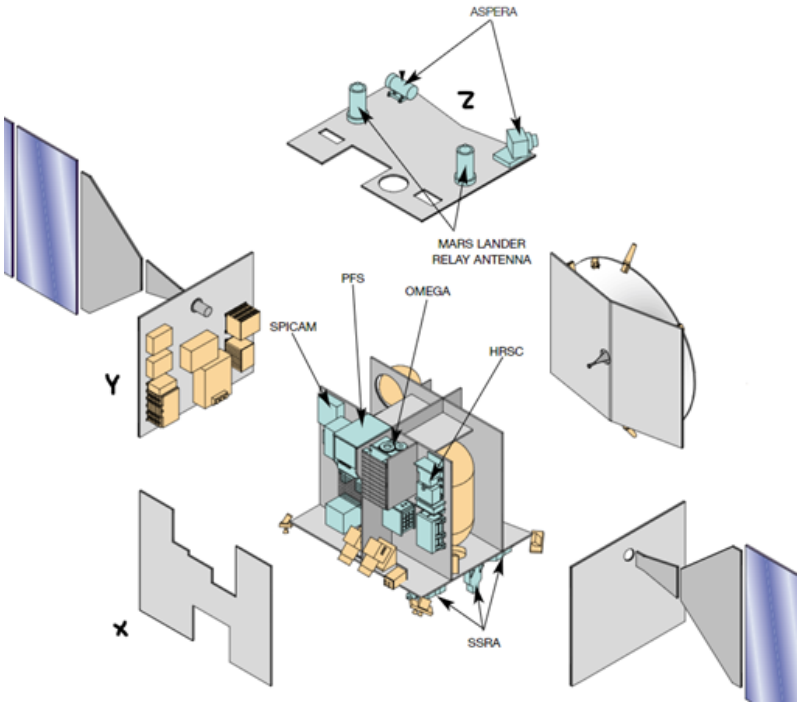

Figure 9.1: Mars Express Structure and configuration, from "ESA's Mars Express Mission– Europe on Its Way to Mars" n.d.

9.1 Structure

The structure is composed by 2 principal sections: A core built from:

- Launch vehicle adapter ring (LVA), made from solid aluminum, D=940mm, h=200mm, t=3.5mm, it's the main load path from launcher to s/c body. (*MEX Instrument overview* n.d.)
- Two tank beams supporting the lower tank part, embedded in the LVA, solid aluminum.
- Two upper tank floors, supporting the upper part of the tanks.
- One lower floor
- Two lateral shear walls in the X direction, One in the Y direction.

An outer structure:

- A top floor, sidewalls.
- Dedicated equipment support panels.

All panels are made from aluminum alloy honeycomb sandwich, 10 to 20 mm thick, with eventual local reinforcing elements. (*MEX Instrument overview* n.d.). Lateral panel supported the avionics and solar arrays, The payload units are allocated following their main needs, the ones needing delicate thermal control and precise pointing (HRSC, OMEGA, PFS, SPICAM) are close to the X shear wall, inside the s/c and close to the ADCS reference (Star sensors and IMU) and thermal radiators, supported by the lateral X walls together with the high gain antenna. The payloads requiring a large field of view are located externally on top and bottom floors (ASPERA), or lower edge of side panels (MARSIS). Beagle 2 was positioned on the top floor in order to reduce the centre of mass displacement in (X,Y) plane, its antenna was positioned nearby. (*MEX Instrument overview* n.d.).

9.2 Requirements

The main high-level requirements regarding the configuration of the spacecraft are:

- The spacecraft must resist the dynamic and static loads during launch phase, for both a Soyuz/Fregat and a Delta II launcher.
- The spacecraft must resist the dynamic and static loads generated by the main engine.
- The structure must be safely connected to the launcher during launch and the loads must be transmitted in the proper way.
- The structure must resist eventual aerobraking solicitations.
- The structure must transmit the loads to all components avoiding excessive solicitations.
- The structure of the spacecraft shall be as light as possible.
- The structure of the spacecraft must be electrically conductive to avoid discharges.
- The Structure must resist to the environmental conditions.
- Development costs of the structure shall be minimized.
- The structure must guarantee the correct alignment of the instruments in every instant.

Bibliography

Litterateur

ArianeGroup (n.d.). *Chemical bi-propellant thruster family Catalog.*

Astrium, EADS (n.d.). *Venus Express Spacecraft Design Report.*

Beagle 2: the Exobiological Lander of Mars Express (n.d.).

Chicarro, A., P. Martin, and R. Trautner (2004). "The Mars Express Mission: An Overview". In: *Mars Express: A European Mission to the Red Planet*. Ed. by Andrew Wilson. ESTEC, Noordwijk, The Netherlands: ESA Publications Division, pp. 3–16.

Collins, Rockwell (n.d.). *RDR 68 Momentum and Reaction Wheels 14 – 68 Nms with external Wheel Drive Electronics Catalog.*

Denis, Michel et al. (2008). "Science Data Management - Comparing Mars Express with Other Missions". In: *SpaceOps 2008 Conference*. DOI: 10.2514/6.2008-3390. eprint: https://arc.aiaa.org/doi/pdf/10.2514/6.2008-3390. URL: https://arc.aiaa.org/doi/abs/10.2514/6.2008-3390.

ESA (n.d.). *concurrent Design Facility Studies Standard Margin Philosophy Description, 2017.*

"ESA's Mars Express Mission– Europe on Its Way to Mars" (n.d.). In: ().

Lavagna, Michèle Roberta (n.d.[a]). *Space System Engineering , Operations course - Exercises, 2022.*

– (n.d.[b]). *Space System Engineering , Operations course - Slides, 2022.*

LOCHE, Didier (2008). *MARS EXPRESS AND VENUS EXPRESS POWER SUBSYSTEM IN-FLIGHT BEHAVIOUR*. DOI: 2008ESASP.661E...4L. URL: https://articles.adsabs.harvard.edu/pdf/2008ESASP.661E...4L.

M. Carranza, V. Companys (n.d.). "Optimisation of the future routine orbit for Mars Express". In: ().

M. Hechler Y. Langevin, A. YáÑez (2005). "Mars Express orbit design evolution". In: *Dynamical Systems.*

M. Lauer S. Kielbassa, U. Herfort (n.d.). "Assessment of ADCS in-orbit performance for Mars Express and Rosetta". In: ().

P. Reginer E. Ecale, S. Val Serra (n.d.). "ADCS Design for scientific missions Rosetta/Mars express". In: ().

Planetary Orbit Insertion – A First Success for Europe with ESA's Mars Express (2006).

"Robust FDI applied to thruster faults of a satellite system" (n.d.). In: ().

Shaughnessy, B. M. (2004). "Development of the Thermal Design for the Beagle 2 Mars Lander". In: *JOURNAL OF AEROSPACE*.

Sodern, ArianeGroup (n.d.). *HORUS, Single-box, standalone Star tracker*.

Space mission engineering : the new SMAD (2011). eng. Space technology library ; v. 28. Hawthorne, CA: Microcosm Press. ISBN: 9781881883159.

SpaceOps 2006 Conference (2006). DOI: 10.2514/6.2006-5857. URL: https://www.researchgate.net/publication/268580724_Mars_Express_Power_Subsystem_In-Flight_Experience.

"The Venus Express Spacecraft System Design" (n.d.). In: ().

Wilson, Andrew, ed. (2004). *Mars Express: A European Mission to the Red Planet*. ESTEC, Noordwijk, The Netherlands: ESA Publications Division. ISBN: 9290925566.

Websites

Beagle 2 (n.d.). URL: https://solarsystem.nasa.gov/missions/beagle-2/in-depth/.

Daniel (n.d.). *KEEPING MEX WARM*. URL: https://blogs.esa.int/rocketscience/2016/10/21/keeping-mex-warm/.

ESA (2001). *HERSCHEL/PLANCK SPACE/ GROUND INTERFACE CONTROL DOCUMENT*. URL: https://www.cosmos.esa.int/documents/12133/1028864/HERSCHEL-PLANCK+SPACE+-+GROUND+INTERFACE+CONTROL+DOCUMENT (visited on 06/26/2022).

– (2022a). *ESA CDF Standard Margin Philosophy*. URL: https://sci.esa.int/documents/34375/36249/1567260131067-Margin_philosophy_for_science_assessment_studies_1.3.pdf (visited on 07/19/2022).

– (2022b). *Mars Express Fact Sheet*. URL: https://sci.esa.int/web/mars-express/-/47364-fact-sheet (visited on 06/26/2022).

MEX Instrument overview (n.d.). URL: https://pds.nasa.gov/ds-view/pds/viewContext.jsp?identifier=urn%5C%3Anasa%5C%3Apds%5C%3Acontext%5C%3Ainstrument_host%5C%3Aspacecraft.mex%5C&version=1.0.

R. Pischel, T. Zegers (2009). *Science planning and operations for Mars Express*. URL: https://sci.esa.int/documents/33745/35957/1567256322922-PREVIEW_MEX_ESA_SP_Science_Planning.pdf.

The Lander: Beagle 2 A

The Beagle 2 project was the probe for the ESA Mars Express mission. The probe consisted of the EDLS and the lander itself initially mounted on the top deck of the Mars Express Orbiter. The Beagle 2 lander objectives were to characterize the landing site geology, mineralogy, geochemistry and oxidation state, the physical properties of the atmosphere and surface layers, collect data on Martian meteorology and climatology, and search for signatures of life. Beagle 2 has no propulsion system of its own and remains attached to Mars Express for much of the journey to Mars. During this time it is substantially shaded from the Sun by the spacecraft, but power is available to heat critical units on the Probe. Although the Beagle 2 successfully separated from the MEX main spacecraft, confirmation of the successful landing never occurred and the mission was declared lost.

The main subsystems of the lander(*Beagle 2* n.d., *Beagle 2: the Exobiological Lander of Mars Express* n.d.) are presented on the following pages: the performed analyses are more qualitative and less precise than the main ones related to the MEX Orbiter. The aim is to provide only a general overview of the system.

A.1 Scientific payload

The lander carries the following sets of instruments and mechanism for in-situ analysis in order to satisfy its mission:

- Sample handling system, robot arm and a mole which can be deployed by the arm and is capable of moving across the surface at a rate of about 1 cm every 5 seconds using a compressed spring mechanism. This mechanism can also allow the mole to burrow into the ground and collect a subsurface sample in a cavity in its tip. The mole is attached to the lander by a power cable which can be used as a winch to bring the sample back to the lander.
- Gas chromatography and mass spectroscopy (GAP) that includes:
  - Microscope, panoramic and wide-angle cameras
  - Mössbauer and X-ray fluorescence spectrometers
  - Environmental sensors

A.2 Mission analysis

The Beagle 2 mission can be divided into the following phases:

- **Cruise and coast**: Beagle 2 was launched with the Mars Express orbiter and was released on a ballistic trajectory towards Mars on 19 December 2003 at 8:31 UT.

The lander coasted for five days after release.

- **Descent**: The lander entered the Martian atmosphere at over 20,000 km/hr on the morning of 25 December. After initial deceleration in the Martian atmosphere from friction, parachutes were to be deployed about 1 km above the surface. Landing was expected to occur at about 02:54 UT on 25 December. Beagle 2 was supposed to land in Isidis Planitia, a plain located in a huge Mars impact basin, the centre of which is at 11.6 ° north latitude and 265° east longitude.
- **Initial lander operations**: After landing the bags would deflate and the top of the lander would open. The top would unfold to expose the four solar array disks. Within the body of the lander a UHF antenna would have been deployed. A panoramic image of the landing area would be taken using the stereo camera and a pop-up mirror. A signal was scheduled to be sent after landing to Mars Odyssey at about 5:30 UT. No signal was received.
- **Operational mission** (180 sols): the lander would perform the scientific operation and then sent them the collected data to the Orbiter during the communication windows.
- **Extended mission**: it was planned a possible extension of the mission of one Martian year

A.3 TMT&TC subsystem

The communication system provides the means for bi-directional UHF radio communication with the Orbiter and NASA's Mars Odyssey. It consists of the following:

- Transceiver (transponder+ interfaces)
- Diplexer, power divider and radio-frequency cables
- Receive and transmit antenna integrated into the lander lid structure.

The data rate provided on the forward link (Orbiter to Lander) are 2 kbps and 8 kbps at a frequency of 437.1 MHz, while the return links work at 2-128 kbps and 401.56 MHz. The telecommunications system is designed to relay at least 10 Mbps per day. The choice of transmitting in UHF it is related to the possibility to obtain relatively compact antennas for reception and transmission that is fundamental in the design of the lander which must be as compact as possible. The Orbiter carried on the MELACOM subsystem: it is a separate UHF radio system, with the primary mission of providing data services for the lander. Mars Express was scheduled to fly over the landing site every 1-4 sols and was to relay scientific data to the UK-based Lander Operations Centre.

A.4 Electric power subsystem

The lander Beagle 2 was powered by a 42-cell Lithium-ion battery (mass 2.63 Kg) module and solar cells. The solar cells were mounted on five deployable panels.The total solar panels area was about 1 m^2 but the front surface of the panels has 85% solar cell coverage. The solar cells were Gallium Arsenide using Germanium substrate (GaAs/Ge) with an 80 micron cover glass, that provide maximum 87 W of power. The common electronics provides the lander with power management and conditioning, power converters, the central processor, descent electronics, pyrotechnic supplies, motor drives, data handling

and experiment interfaces. The electronics are robust and failure-tolerant as there is no redundancy in the system due to mass-restrictions.

After the separation, the Beagle 2 must rely on its own battery, which cannot last beyond 6 days, until its solar arrays are fully deployed on the surface. The battery shall provide energy also for the night-time operations during the nominal lifetime of the mission of 180 sols. The duration of a Martian day is 24 h 39 min, and it was supposed that the night duration has an average of 10 h since the landing site is near to the Mars equator.

The payload needs a power less than 40 W. No more precise information are available, so for this reason the following assumption were made:

- The maximum power demand is 40 W
- The maximum power demand in daylight and nigh-time is the same
- A 10% of margin is applied at the total power demand

The maximum power demand is resulted 44 W. The same approaches used for the analysis of the Orbiter power subsystem was used for the lander; for this reason the complete procedure is not reported, but only the main considerations and the results.

A.4.1 Solar panels sizing

It was supposed a direct energy transfer (X_e=0.65 and X_d=0.85) configuration because it is simpler and lighter. This is in accordance with one of the main driver for the realization of the lander that is the mass reduction, in order to be compliant with the launcher mass requirement. The assumed main inefficiency were:

- Inherent loss: I_d=0.77
- Cosine loss: α=12°
- Gallium-Arsenide cell efficiency: η=30%
- Degradation factor: d=3.75% per year

The results obtained are reported in Table A.1:

Results

		Estimated	Real
P_{sa}	[W]	115.97	87
P_0	[W/m^2]	147	-
P_{BOL}	[W/m^2]	110.7	-
P_{EOL}	[W/m^2]	108.6	-
A_{sa}	[m^2]	1.068	0.85

Table A.1: Beagle 2: Solar panels sizing results

The area and the obtained power result a bit high with respect to the real one, but as expected, the estimation was not very precise due to lack of data regarding the power demand of the subsystem. Assuming a specific power equal to 70 W/kg accordingly to the choice of the solar cells a mass of 1.66 kg was obtained.

A.4.2 Battery sizing

It was supposed to use Li-ion battery with E_d=125 Wh/kg and with the same feature of the cell used for the Orbiter like the real mission. The main initial data are collected in

the Table A.2.

Results		
E	[Wh]	440
Mission lifetime	[year]	0.493
Total cycles	[-]	180
DOD	[-]	98%
Efficiency	[-]	0.95
Cell capacity	[Ah]	1.5
Cell voltage	[V]	4.2
Bus voltage	[V]	28

Table A.2: Beagle 2: Battery data

The results are summarized below in Table A.3.

Results			
		Estimated	Real
C_r	[Wh]	472.6	200
C_r	[Ah]	16.87	-
N_{ser}	[-]	7	-
V_{real}	[V]	29.4	-
C_{string}	[Ah]	35.28	-
N_{string}	[-]	14	-
C_{real}	[Ah]	493.9	-
$Mass$	[kg]	3.5	2.6

Table A.3: Batteries sizing results

The resulting number of total cells is 98: the value is more than the double of 42 (the real value), and moreover also C_r results more than the double of the real value of about 200 Wh. The main reasons of these results are in the term E because first, the power demand in eclipses was unknown and there was only a coarse information about the maximum power demand, and moreover there was not precise information about the duration of the night on Mars that changes also accordingly to its distance from the Sun following its high eccentric orbit.

In addition to the more general requirements, it is necessary to add that the EPS subsystem shall withstand and cope with a highly variable and adverse environment (dust storms, large temperature differences).

A.5 Thermal control subsystem

The thermal design of the Probe has been driven largely by the Coast phase temperature requirements. During Coast, the operational temperature requirements of the Entry, Descent, and Landing System must be achieved passively. The battery and the AGS in particular have tight operational temperature limits; The thermal design for Coast therefore relies upon optimization of the surface finishes and insulation to control the absorbed solar energy:

- MLI blankets are applied to the frontshield and to the conical backshell.

- The frontshield MLI has a black kapton external layer. This serves also to radiate the heat absorbed during launch.
- The backshell MLI has a vacuum deposited aluminum external surface.
- The frontshield is radiatively decoupled from the Lander by an aluminized coating on its inner surface. This reduces heat loss from the Lander and minimizes the temperature of the frontshield thermal protection

The primary thermal design driver for the Lander is the Martian environment at the landing site and during the period of planned operation. The Lander has the following environmental boundary conditions:

- Absorption of direct and diffuse solar radiation.
- Radiative losses to the effective sky temperature.
- Radiative losses to the surrounding Martian surface.
- Convective losses to the nearby atmosphere
- Conductive losses at the thermal interface between the underside of the Lander and the Martian surface.

The landing site was selected in part due to thermal constraints on latitude. The time of landing is shortly after the major dust storm season, so there could still be a significant level of dust left in the atmosphere. During dust storms the optical depth decrease and this impacts on the proportion of direct solar radiation reaching the surface, the proportion of scattered solar radiation reaching the surface and the effective sky radiation temperature. Dust coverage also modifies the thermo-optical finishes of the Lander external surfaces. The battery had the tightest temperature limits and thus became the major thermal design driver. For this reason power system and batteries were kept in an insulated warm compartment. In addition, thermally absorbing materials were applied to transfer the heat of the sun into the battery compartment during daytime to ensure that the power system did not cool down too low during night-time. Items outside of the Lander compartment (for example, instrument arm, solar arrays) were qualified to survive the extreme cold temperatures experienced overnight that can reach -80°C. (Shaughnessy (2004))

A.6 Configuration

The main compartment of the Lander is roughly saucer- shaped, having an external diameter of about 650 mm and a depth of 250 mm. The compartment is constructed as an inner and outer skin separated by Rohacell foam, which provides both thermal insulation from the Martian environment and impact protection for the landing. The inside of the Lander is divided into three 120° segments. One segment contains the battery and common electronics. A second contains a miniature gas analysis package (GAP). The base of the robotic arm is mounted within the third segment, which also provides space to stow the suite of science instruments (the PAW) that are fitted to the end of the robotic arm. When stowed, the robot arm folds into a recess between the battery and GAP.

The main high-level requirements regarding the configuration of the Lander are:

- The lander structure must be capable of resisting all static and dynamic loading conditions transmitted from the spacecraft.
- The lander structure must be capable of resisting atmospheric re-entry conditions.
- The lander structure must be capable of resisting the impact with Mars' surface.